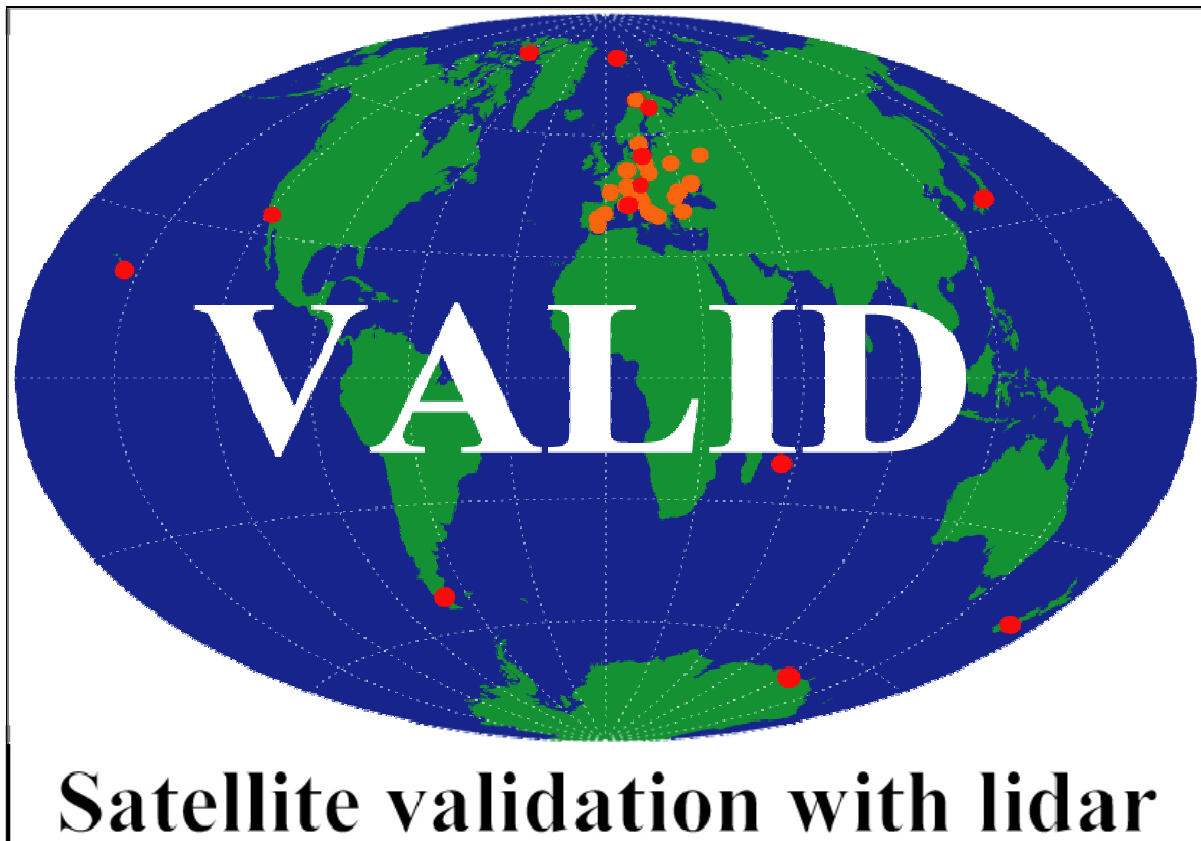


Annual Report

2008



Prepared by: Anne van Gijssel (RIVM), Felicita Russo (CNR-IMAA),
Gelsomina Pappalardo (CNR-IMAA) and Daan Swart (RIVM)
Reviewed by: Thorsten Fehr (ESA), Yasjka Meijer (ESA) and Ewa Kwiatkowska
(ESA)
Issued on: 18-02-2009
Contract no: 18193/04/NL/AR

Table of Contents

1	Summary.....	4
2	Introduction.....	6
2.1	Ozone and temperature profiles	6
2.2	Aerosol and cloud lidar data.....	6
2.3	Organisation of this document	8
3	LIDAR Data.....	9
3.1	Ozone and temperature lidar – status per site	9
4	Data availability and validation approach.....	13
4.1	ENVISAT data availability	13
4.2	Identification of satellite-derived aerosol and cloud products for validation and climatological studies.....	14
4.2.1	MODIS	14
4.2.2	OMI.....	15
4.2.3	CALIPSO	17
4.3	Validation approach.....	19
4.3.1	Strategies for validation of ozone and temperature profiles derived from satellite measurements	19
4.3.2	Strategies for validation of cloud and aerosol products from satellite measurements	20
4.3.3	Software development	21
5	SCIAMACHY	22
6	MIPAS.....	26
7	GOMOS.....	28
8	MODIS.....	31
9	CALIPSO.....	34
10	VALID-related presentations and publications	36
11	Conclusions	37
12	References.....	38
13	Appendix 1: The EARLINET database.....	42
13.1	Database content.....	42
13.1.1	Single profile file NetCDF structure	43
13.1.2	Timeseries NetCDF file structure	44
13.2	File naming conventions	45
13.3	Database organization	45
13.4	Definition of the parameters	46
14	Appendix 2: Overview of submission statistics - tables.....	48

1 Summary

This is the annual report of the VALID project. In 2008 this project has supported and performed the quality assessment of ozone and temperature profiles retrieved from ENVISAT data using lidar data. This part of the project is coordinated by RIVM and is the Multi-Mission successor of the Envisat Quality Assessment with Lidar project (EQUAL, 2003-2007). New in the VALID project is the comparison of operational cloud and aerosol products from satellites with measurements performed by ground-based lidars in EARLINET. This part is coordinated by CNR-IMAA. The report is therefore naturally split into two main components: (1) ozone and temperature profiles (largely in the stratosphere resp. stratosphere and mesosphere) and (2) cloud and aerosol properties (largely in the troposphere). As the cloud and aerosol part is new, somewhat more text is devoted to this subject.

3832 ozone profiles and 4305 temperature profiles over the period 2002 to 2008 have been submitted so far.

GOMOS ozone profiles (IPF 5.00/GOPR 6.0) have already shown an excellent agreement with lidar data with a bias within 5% between altitudes of 18–45 km. Verification of version GOPR 7 indicated few differences with version 6 for the ozone profiles. The comparison of high-resolution temperature product (HRTP) for these two versions hints at an improvement except at the top of the version 7 profiles which pointed out an initialisation problem. Note that very few HRTP data were available for both versions. More data and further corrections are therefore recommended.

MIPAS optimised resolution (OR, formerly known as “reduced resolution” - RR) had no operational level 2 data processing in the reporting period. Instead, we have carried out a preliminary analysis on scientific data from Oxford University (MORSE versions 1.00, 1.01 and 1.02). Selected datasets of June 2007 to January 2008 were tested. Unfortunately, the three versions have not processed the same MIPAS dataset, so they cannot be compared directly. It is clear that progress is made with the sequential versions where for version 1.02 the ozone profiles match up very well to the lidar profiles from 18 km up to an altitude of 30 km. Above this altitude, the algorithm starts to overestimate the ozone concentration to reach a maximum overestimation around 40 km where the median deviation is about 20%. We also notice some outliers around this altitude.

Temperature profiles from version 1.02 were compared with sonde, microwave and lidar data. A deviation with a peculiar shape is seen around 30 km, but for most altitudes, data is within 1 Kelvin.

SCIAMACHY ozone profiles from operational processor version 3.01 were found to underestimate the ozone concentration around the ozone maximum, but within 20% deviation, which is in line with our previous validations. In a verification study using a limited dataset, various candidate-processors for version 4.x were found to have significantly improved ozone estimations around the ozone maximum. In 2008 we also started to assess data produced by the scientific algorithm Stratozone 2.0 from IUP Bremen; this validation will be completed in 2009 with the application of the provided averaging kernels.

The involvement of EARLINET in the VALID activities concerns the analysis and the report of the quality of the aerosol and clouds measurements of ESA’s and third-party atmospheric sensors (e.g., CALIPSO, ADM-AEOLUS, EarthCARE). In the first year of the VALID project CNR-IMAA surveyed and studied the major satellite products identifying the aerosol measurements suitable for comparison with lidar measurements, focusing initially on CALIPSO, MODIS and OMI products. Some comparisons between lidar and satellite aerosol measurements were performed. In particular an example of climatological comparison between AOD measurements

obtained with the Raman Lidar PEARL (Potenza EARlinet Lidar) and measurements obtained with MODIS is presented as well as a point-to-point comparison with profiles of attenuated backscattering obtained with CALIPSO. CNR-IMAA also studied the format of the data to be submitted to the ESA calibration/validation database at NILU, generating complementary codes to prepare the EARLINET data for the conversion to HDF.

2 Introduction

This is the annual report of the *Satellite validation with lidar* (VALID) project led by the Dutch National Institute for Public Health and the Environment (RIVM) with a sub-contract to the Italian National Research Council – Institute of Methodologies for Environmental Analysis (CNR-IMAA). The objectives of this project have been to provide the European Space Agency (ESA) with adequate support for the assessment and reporting on the product quality of temperature and ozone profiles retrieved from ENVISAT data in the period 2008-2010 and secondly, to study the possibilities of using EARLINET lidar data for the validation of aerosol and cloud products from satellite-borne sensors.

2.1 Ozone and temperature profiles

In order to fulfil the first objective, temperature and ozone profiles obtained with stratospheric lidars from a total of 13 stations (see Figure 1) have been collected and made accessible for comparison.

Lidar systems used in the long-term validation of ENVISAT ozone/temperature profiles

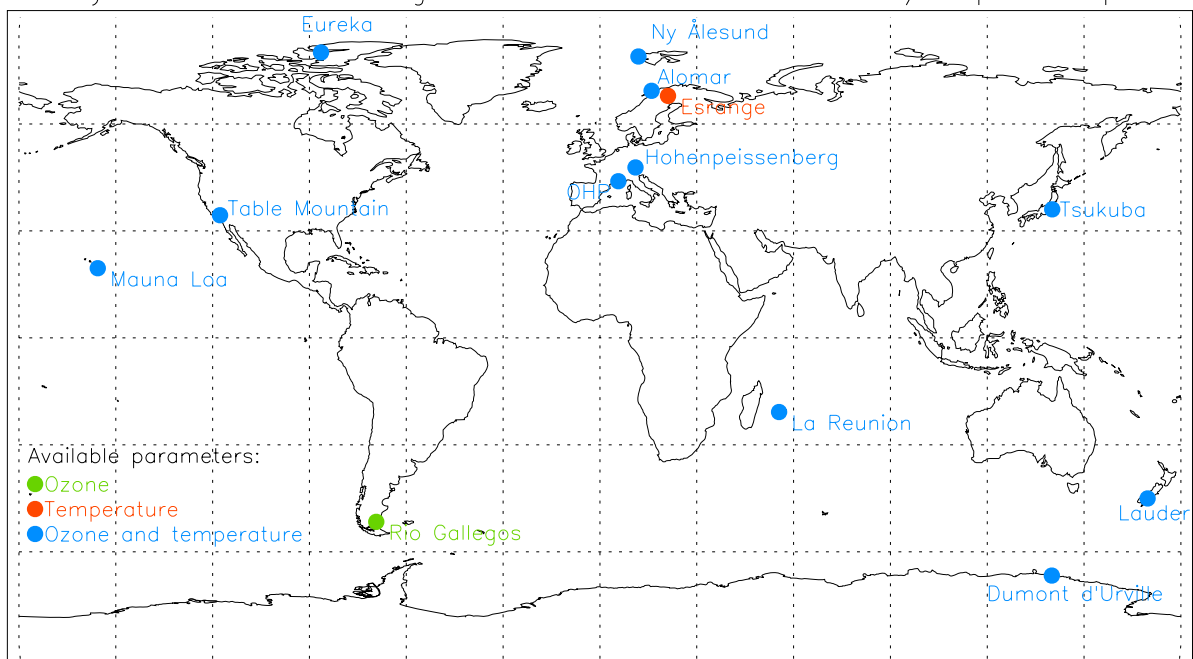


Figure 1: Station locations of the lidar instruments used in the VALID project for validation of ozone/temperature profiles.

2.2 Aerosol and cloud lidar data

Aerosol and cloud lidar profiles have been added to the project in 2008.

Aerosols play an important role in the climate system and their effect is one of the major uncertainties of present climate predictions (Forster et al., 2007). Aerosols play also a major role in atmospheric chemistry affecting the concentrations of other potentially harmful atmospheric constituents like ozone. Furthermore they are an important controlling factor for the radiation budget, in particular in the UV-B part of the spectrum. When at ground level, some kind of aerosols can be harmful, even toxic, to man, animals, and plants. For all these reasons it is necessary to achieve an advanced understanding of the processes that generate, redistribute, and remove aerosols in the atmosphere. Satellite imaging of aerosols, coupled with radiation measurements, is very important for the study of the role of aerosols on global climate change. Satellites could in fact help to track the evolution of aerosol plumes, dust storms, forest fires and anthropogenic aerosols giving a global image of the aerosol distribution around the globe. The

vertical distribution of aerosols is however a key parameter for the study of their evolution in the atmosphere. This strongly depends on their vertical location. Combining satellite measurements with vertically resolved measurements (in particular high vertical resolution profiles such as those measured by lidar) is a necessary strategy for the full understanding of aerosol evolution processes. In particular, a quantitative dataset describing the aerosol vertical, horizontal, and temporal distribution, including its variability on a continental scale, is necessary. Such dataset, besides increasing our knowledge of aerosol emission and removal processes, could be used to validate and improve models that predict the future state of the atmosphere and its dependence on different scenarios. An improvement of the prediction models would have, as a major consequence of large interest, the ability to define the necessary actions to be taken to preserve the quality of the environment. No suitable data set for this purpose presently exists (Bösenberg et al., 2003). The creation of such database represents the principal motivation for the constitution of the EARLINET network (European Aerosol Research Lidar Network) (Bösenberg et al., 2003). EARLINET was established in 2000 as a research project supported by the European Commission under the Fifth Framework Programme with the main goal to establish a quantitative comprehensive statistical database of the horizontal, vertical, and temporal distribution of aerosols on a continental scale. Its objective is to provide aerosol data with unbiased sampling, for important selected processes, and air-mass history, together with comprehensive analyses of these data. A very important activity within this network is to ensure data quality, for which a dedicated program has been defined within the infrastructure. Since aerosol distribution and composition vary during the day and with the season, in order to establish a significant database for the study of aerosol climatology the measurements are performed according to a fixed schedule. Additional measurements are performed to specifically address important processes that are localised either in space or time. Back-trajectories derived from operational weather prediction models are used to characterise the history of the observed air parcels, accounting explicitly for the vertical distribution.

After the end of the EARLINET project in 2003, the network activity continued on the base of a voluntary association until March 2006, when the EC project EARLINET-ASOS (Advanced Sustainable Observation System) started on the base of the EARLINET infrastructure (Amodeo et al., 2007).

The EARLINET-ASOS project will contribute to the improvement of continuing observations and methodological developments that are needed for providing the multi-year continental scale dataset necessary to assess the impact of aerosols on the European and global environment and to support satellite missions. The main goal is to improve the EARLINET infrastructure with high quality aerosol data and therefore the optimization of the algorithms for the retrieval of aerosol optical and microphysical properties is a crucial activity. The main activity within EARLINET-ASOS is to provide all partners with the possibility to use a common processing chain for the evaluation of their data, from raw signals to final products. Raw signals may come from different types of systems, and final products are profiles of aerosol optical properties, such as aerosol backscattering and extinction coefficients, and in some cases aerosol microphysical properties. The availability of such dataset will have a strong impact on the scientific community since such data with homogeneous and well characterised quality level will be made available for the first time.

EARLINET currently consists of 25 lidar stations (Figure 2). It contains eight multi-wavelength Raman lidar stations that are used to retrieve aerosol microphysical properties, eight Raman lidar stations and nine elastic-backscatter lidar stations.

The main activity of the CNR-IMAA group in this first year of the VALID project has been the identification of satellite products that are suitable for comparison studies with the Raman lidar measurements of aerosols and clouds. In chapters 8 and 9 we will describe the selection of satellite products for such purpose.

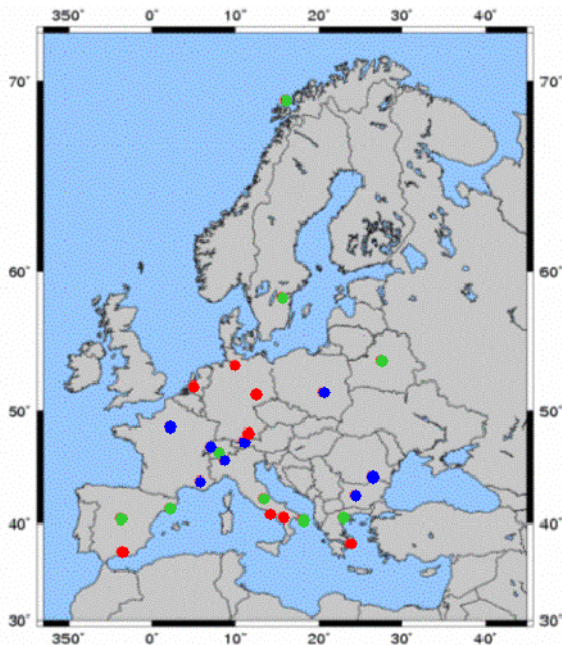


Figure 2: Map of Europe with all the EARLINET lidar stations: (red circles) multi-wavelength Raman lidar stations; (blue circles) Raman lidar stations; (green circles) elastic-backscatter lidar stations

In particular the following tasks were involved:

- Performance of lidar measurements at the locations of the EARLINET partner institutes.
- Lidar data processing for the retrieval of aerosol and/or cloud properties.
- Checking of data quality.
- Data formatting to comply with ESA's calibration/validation database.
- Uploading of all correlative measurements to the calibration/validation database.
- Request and download satellite data.
- Understanding and reading of satellite data.
- Derive lists of collocated measurements between satellite and lidar observations.
- Perform comparison studies between satellite and lidar profiles of aerosol and clouds.
- Report to applicable groups during meetings/conferences.
- Contribute to the reporting by RIVM (validation reports, annual reports, final report).

In the first year of the VALID project CNR-IMAA:

- Surveyed and studied the major satellite products identifying the aerosol measurements suitable for comparison with lidar measurements.
- Requested and downloaded of some of the identified products.
- Performed some comparisons between lidar and satellite aerosol measurements.
- Studied the format of the data to be submitted to the ESA calibration/validation database at NILU.
- Generated complementary codes to prepare the EARLINET data for the conversion to HDF.
- Successfully converted some EARLINET example files.

2.3 Organisation of this document

Chapter 3 provides an overview of the available measurements that were submitted to the correlative database maintained at NILU. This document continues with the availability of the ENVISAT data and the validation approach in chapter 4. The validation activities carried out are subsequently presented for SCIAMACHY (chapter 5), MIPAS (chapter 6), GOMOS (chapter 7), comparison of aerosol optical depth for MODIS (chapter 8) and finally the profile comparison between the CNR-IMAA EARLINET lidar and CALIPSO (chapter 9). The last chapters give an overview of VALID-related publications (10) and present the conclusions (11).

3 LIDAR Data

For aerosol and cloud properties, data is collected from the EARLINET infrastructure which consists of 25 stations (Figure 2). The EARLINET infrastructure represents a unique tool in the VALID activity for the validation of aerosol and cloud optical properties retrieved from satellites.

Thirteen lidar stations in the VALID network are collecting ozone and/or temperature profiles (see Figure 1 and Table 3-1). The statistics of the lidar data that have been measured, processed, converted (to HDF) and submitted to the ENVISAT Cal/Val database (maintained by NILU) are shown in Figure 3 for the ozone profiles and in Figure 4 for the temperature profiles. Each figure presents per month the number of days with lidar measurements. Note that multiple profiles per day are counted as one in this representation. The first set of panels regard the ozone measurements, while the second part concerns the temperature measurements. In each panel title we have indicated with an acronym the station location (see Table 3-1) and the system name which corresponds to the filename in the NILU database (e.g., files with NILU001 in their name contain ozone profile information and NILU002 temperature profile information, and both for the Alomar research facility, Norway).

Ground station	Acro	Lat.	Long.	Parameter	System name
Eureka	EUR	80.05	-86.42	Ozone, temperature	CARE.STB.EC001, CARE.STB.EC002
Ny Ålesund	NYA	78.92	11.93	Ozone*, temperature	AWI001, AWI002
Alomar	ALO	69.30	16.00	Ozone, temperature	NILU001, NILU002
Esrange	ESR	67.88	21.10	Temperature	UBONN003
Hohenpeissenberg	HOH	47.80	11.02	Ozone, temperature	DWD001, DWD002
Obs. Haute Provence	OHP	43.94	5.71	Ozone, temperature	CNRS.SA001, RMR_CNRS.SA001
Tsukuba	TSU	36.05	140.13	Ozone, temperature	NIES001, NIES002
Table Mountain	TMF	34.40	-117.70	Ozone, temperature	NASA.JPL003, NASA.JPL004
Mauna Loa	MLO	19.54	-155.58	Ozone, temperature	NASA.JPL001, NASA.JPL002
La Reunion	LAR	-20.80	55.50	Ozone, temperature	LPA001, LPA002
Lauder	LAU	-45.04	169.68	Ozone, temperature	RIVM002, RIVM003 [#]
Rio Gallegos	RGGA	-51.6	-69.3	Ozone	CEILAP001
Dumont d'Urville	DDU	-66.67	140.01	Ozone, temperature	CNRS.SA007 [#] , RMR_CNRS.SA002 [#]

* In the new project (VALID), only temperature data will be available.
[#] Data is being validated and not yet available, see also section 3.1 below

3.1 Ozone and temperature lidar – status per site

The section below discusses the data processing and physical status of each ozone/temperature lidar.

No specific problems have been reported for **Eureka**. The site will host the bi-annual NDACC lidar working group meeting in 2009.

In 2008, the project contacts for the **Ny Ålesund** site (Ronald Neuber and Peter von der Gathen) indicated that they would not be able to commit to ozone measurements with lidar in

the new VALID project. Profiles for part of the EQUAL-period have been measured, but as result of a focus change, processing has got a low priority. For the VALID project, our new contact is Marion Maturilli, responsible for the temperature retrieval with a Rayleigh lidar. She has indicated that for 2008 about 30 profiles can be expected.

In **Alomar**, a new Licel detector system was installed in March 2008. This should increase the quality of the profiles, but also required an adjustment of the analysis software. Data for the period March to December 2008 (15-20 profiles) is still undergoing validation.

Operation and management of the **Esrangle** lidar have moved from the supervisor by Universität Bonn to the Esrangle Space Center and the Meteorological Institute of Stockholm University. The latter has hired a PhD student to process the lidar measurements. Measurements were performed on 23 days in 2008.

The lidar at **Hohenpeissenberg** is in a good condition.

The acquisition system of the ozone lidar at **Observatoire Haute Provence** has been changed in June 2008. Noise was found in the new data, so filtering is required and validation is still taking place.

The temperature lidar was unavailable for 3 months in 2008 due to problems with the acquisition system.

Temperature data series for **Tsukuba** have been updated as the station elevation was not included in the reported altitude. Data submission (ozone and temperature) for the remaining months of 2008 is expected this April.

The lidar at **Table mountain** is performing well after experiencing various problems in 2007.

The lidar at **Mauna Loa** is in a good condition.

The ozone lidar at **La Reunion** experienced consecutive severe hardware failures in the period 2007-2008. Measurements have been resumed at end of 2008, but data are still awaiting validation. The temperature lidar has had a few problems, but has been operational for most of the period.

The **Lauder** system is performing well. Temperature retrieval is not yet operational, but this work will be continued in 2009.

The lidar at **Rio Gallegos** is in a good condition.

Large maintenance was performed at **Dumont d'Urville** in 2009. The system should be operational. No data has been received yet.

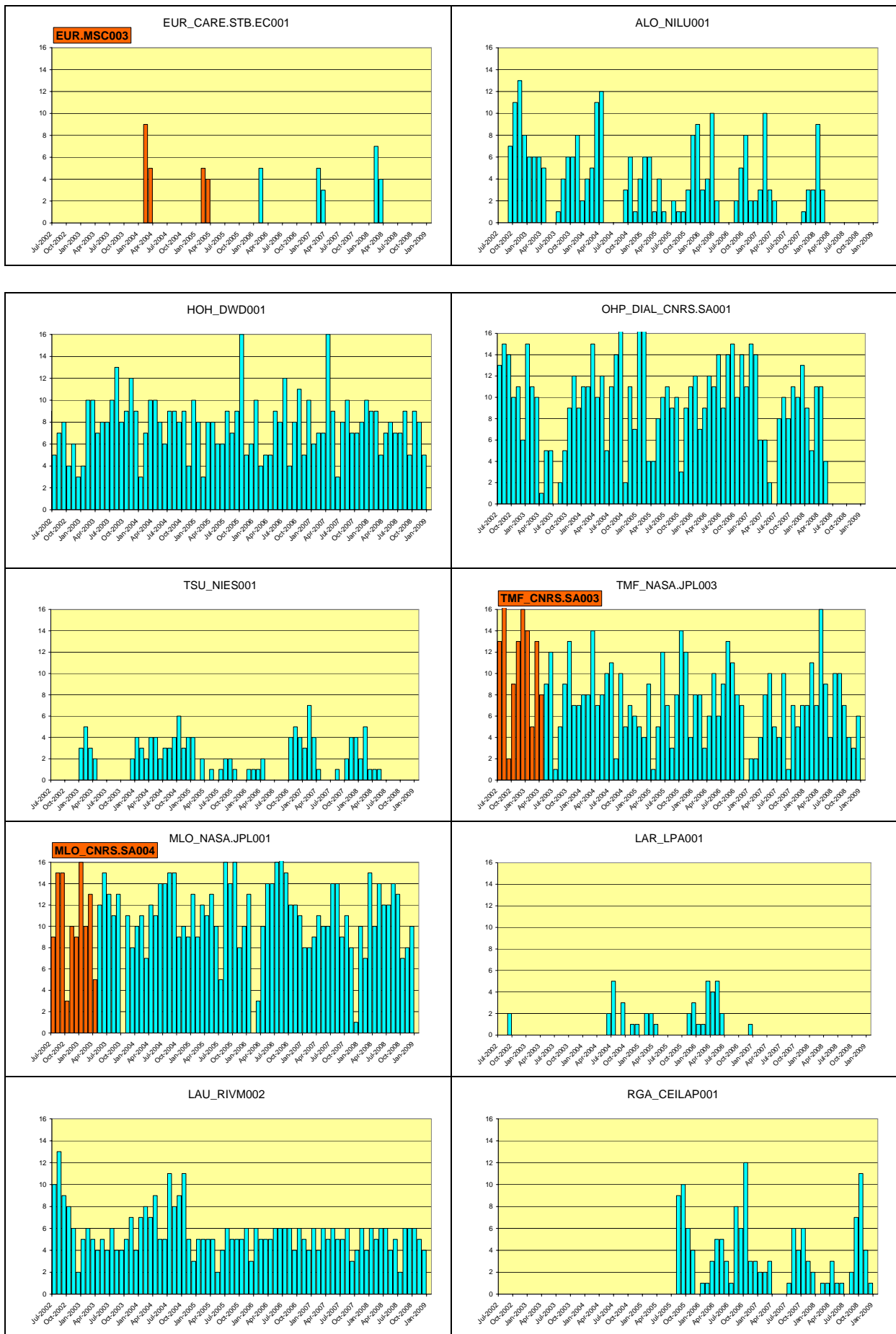


Figure 3: Statistics of available OZONE lidar data in the NILU database. Numbers indicate the number of days per month with lidar measurements. Note that the maximum range for the numbers is fixed to 16 and larger numbers are not displayed (see Tables 14-1 – 14-6).

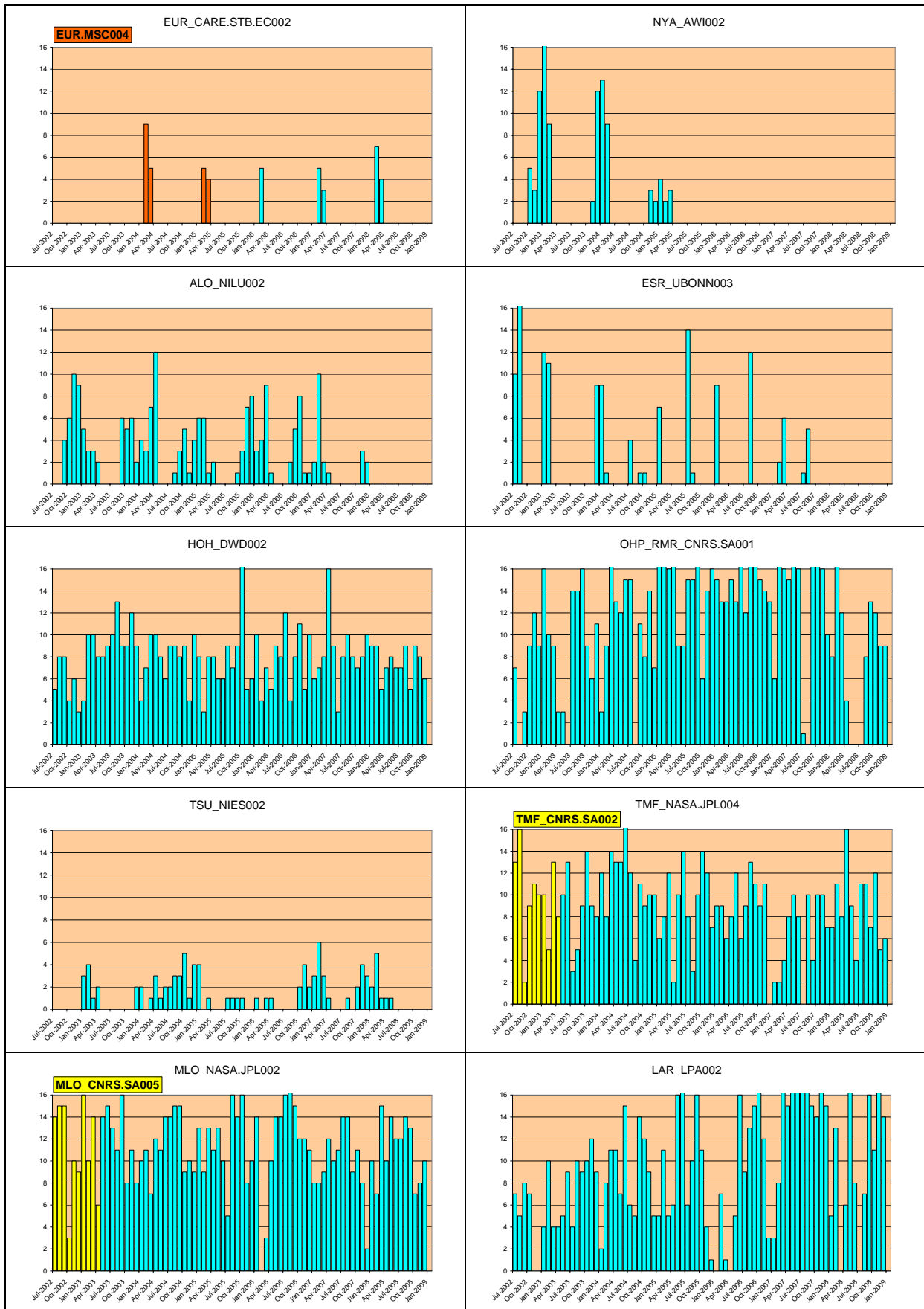


Figure 4: Statistics of available TEMPERATURE lidar data in the NILU database. Numbers indicate the number of days per month with lidar measurements. Note that the maximum range for the numbers is fixed to 16 and larger numbers are not displayed (see Tables 14-1 – 14-6 for these values).

4 Data availability and validation approach

4.1 ENVISAT data availability

In this section we give an overview of the available ENVISAT data (level 2) for the VALID project (see Table 4-1, Table 4-2 and Table 4-3). Note that data might have been (temporarily) available but not acquired within the VALID project. These tables serve as a rough indication and they are not a precise representation of actual data availability.

Legend: = potential data, = available data							
Table 4-1: Available ENVISAT Data from IPF Processor							
<i>Instrument</i>	2002	2003	2004	2005	2006	2007	2008
GOMOS
MIPAS	OR-mode.....
SCIAMACHY

Table 4-2: Available ENVISAT Data from Prototype Processor							
<i>Instrument</i>	2002	2003	2004	2005	2006	2007	2008
GOMOS
MIPAS	OR-mode.....
SCIAMACHY

Table 4-3: Available ENVISAT Data from Scientific Institutes							
<i>Instrument</i>	2002	2003	2004	2005	2006	2007	2008
GOMOS*
MIPAS	OR-mode.....
SCIAMACHY

* As enough GOMOS data are available through the nominal ESA processing chain, no 'scientific' datasets were obtained.

4.2 Identification of satellite-derived aerosol and cloud products for validation and climatological studies

Satellite measurements of aerosol and cloud properties are very important for the study of the global role that they have on climate. Satellite measurements have the important advantage to provide a global knowledge of the aerosol and cloud distribution and evolution which is impossible to reach using only ground based instruments. The advantage of lidar is the ability to accurately measure the vertical distribution of aerosols and clouds. The combination of satellite measurements with the measurements obtained within an infrastructure such as EARLINET allows combining the advantages of both techniques. From this combination it will be possible to create a three-dimensional dataset of aerosol and cloud properties.

In the framework of this project we have surveyed the satellites that are currently operational in search for the products that are suitable for the comparison with lidar measurements. The main requirement for this selection was to have satellite measurements of physical quantities, such as the aerosol optical depth that can be directly compared with Raman lidar measurements. The major satellites that retrieve aerosol optical depth and aerosol optical properties have been considered and for the time being three satellite instruments were identified as having aerosol products suitable for the comparison with lidar measurements: MODIS, OMI and CALIPSO. At present these represent the most widely used satellites for aerosol measurements. In the work to follow other satellites and instruments (such as MERIS, SCIAMACHY and GOMOS) could be considered and their aerosol and clouds products suitability for comparison with Raman lidar data will be evaluated. The validation strategy studied during VALID will be useful to current and future ESA missions (ADM-Aeolus, EarthCARE).

In the following sections we give a description of each satellite and corresponding product while in chapters 8 and 9 we give examples of possible studies using this kind of measurements combined with Raman lidar measurements.

4.2.1 MODIS

The MODerate Resolution Imaging Spectroradiometer (MODIS) is a major instrument on the Earth Observing System TERRA (EOS-AM1) and AQUA (EOS-PM1) missions (King et al., 1995). MODIS has the capability to observe nearly the entire earth every two days and provide key observations important to studies of the atmosphere, oceans, and land surfaces (Barnes et al., 1998). MODIS collects images in 36 spectral bands between 0.412 and 14.235 microns with spatial resolutions of 250 m (2 bands), 500 m (5 bands), and 1000 m (29 bands). These bands have been carefully selected to enable advanced studies of land, ocean, and atmospheric processes (King et al., 1992, Running et al., 1994, Salomonson et al., 1991, Gordon, 1990, Gordon et al., 1983, Susskind et al., 1984).

The MODIS instrument is designed to scan through nadir perpendicularly to the velocity vector of the spacecraft, with the maximum scan extending up to 55° on either side of nadir. At the orbital altitude of 705 km this corresponds to a swath width of 2330 km centred on the satellite ground track. Each spectral band detector is aligned parallel to the other detectors so that a single scan of the scan mirror images on the focal plane, a swath of 10 km in the direction of the track. The large number of bands allows retrieving aerosol optical depth over the different types of surfaces. Different methods for deriving the aerosol optical depth are used and can be classified into two categories, called methods of the first and second type (King et al., 1992).

In methods of the first type the aerosol optical depth can be determined from reflection function measurements in a single image. This method allows the retrieval of aerosol optical depth over surface covers that have low spectral reflectance and requires the surface reflectance to be known a priori. In the blue wavelength region of MODIS (0.42 and 0.47 μm), the aerosol optical depth can be determined over vegetation, dark soils, and water bodies with low chlorophyll and low

turbidity; in the red region (0.66 μm) over dark densely vegetated forests and large water bodies; and in the near-infrared (0.87, 1.24, 1.64 and 2.13 μm) over large water bodies (King et al., 1992). In methods of the second type the difference in optical depth is derived from the change in the measured contrast between pixels of the image. This method has the advantage of allowing the retrieval of the optical depth even in absence of dark pixels, but it makes it difficult to convert the retrieved differences into absolute optical depth. These methods are used to retrieve aerosol optical depth over land (King et al., 1992). Therefore the aerosol optical depth in the blue wavelength region has been identified as suitable for comparison with Raman lidar measurements.

In chapter 8 we will present the results of the first statistical comparison of the aerosol optical depth between MODIS and one of the EARLINET Raman lidar stations.

4.2.2 OMI

The Ozone Monitoring Instrument (OMI) instrument is a nadir viewing imaging spectrograph that measures the solar radiation backscattered by the Earth's atmosphere and surface over the entire wavelength range from 270 to 500 nm with a spectral resolution of about 0.5 nm. It is onboard the EOS-Aura satellite and the 114° viewing angle of the telescope corresponds to a 2600 km wide swath on the surface, which enables measurements with a daily global coverage. The light entering the telescope is depolarised and then split into two channels: the UV channel (wavelength range 270 – 380 nm) and the VIS channel (wavelength range 350 – 500 nm). In the normal global operation mode, the OMI pixel size is 13 km \times 24 km at nadir (along \times across track). In the zoom mode the spatial resolution can be reduced to 13 km \times 12 km. The small pixel size enables OMI to look in between of the clouds, which is very important for retrieving tropospheric information (Royal Netherlands Meteorological Institute (KNMI), 2008).

OMI combines the spectrometric advantages of GOME and SCIAMACHY with the advantages of TOMS, measuring the complete spectrum in the ultraviolet/visible wavelength range with a very high spatial resolution (13 km \times 24 km) and daily global coverage (Royal Netherlands Meteorological Institute (KNMI), 2008).

The OMI products that were identified as suitable for the comparison with the Raman lidar are: **OMAERUV** (aerosol absorption optical depth and single scattering albedo) and **OMAERO** (aerosol absorption optical depth and aerosol types)

OMAERUV

The OMAERUV algorithm is used to characterize the atmospheric aerosol load. Based on the TOMS UV algorithm, the OMAERUV algorithm derives the aerosol index (AI), aerosol absorption optical depth (AAOD), and the aerosol optical depth (AOD) at 354, 388 and 500 nm. The optical depth values at 388 nm are inverted from radiance observations while the 354 and 500 nm results are obtained by conversion of the 388 nm retrievals (National Aeronautics and Space Administration (NASA), 2007). This conversion is performed to allow comparisons with other satellite sensors. However, the transformation from 388 nm to 354 and 500 nm increases the dependence of the algorithm on the assumed model of aerosols, so the reported values at wavelengths other than 388 nm, particularly those at 500 nm, should be considered less reliable (National Aeronautics and Space Administration (NASA), 2007). Because of the large sensitivity of OMI near UV observations to particle absorption, the AAOD is the most reliable quantitative OMAERUV aerosol parameter. AAOD is by definition insensitive to clouds, therefore the AAOD retrieval can be applied even in case of cloud contamination and is not restricted to completely cloud-free scenes as it is the case for the AOD retrieval (National Aeronautics and Space Administration (NASA), 2007).

In scenes with prevailing cloud free conditions, the AOD can be reliably retrieved. For example cloud interference with satellite retrieval is negligible over arid and semi-arid regions where dust aerosols are commonly present. In the case of biomass burning and forest fires the accuracy of

the AOD retrieval depends on the vicinity of the source. In fact as the plumes of dust and smoke aerosols drift away from their source regions, they mix with clouds and the OMAERUV AOD retrieval becomes more difficult.

The OMAERUV aerosol algorithm currently uses the measurements made at just two wavelengths: 354 and 388 nm. This is partly to maintain heritage with similar algorithm used for TOMS, and partly because of lack of reliable surface reflectance data at the longer OMI wavelengths. Wavelengths below 340 nm cannot be used due to strong ozone absorption (National Aeronautics and Space Administration (NASA), 2007).

The main advantage of using the near-UV technique as opposed to the IR techniques for deriving aerosol AOD is that in this wavelength region the reflectance of all terrestrial surfaces is very low, and the retrieval of aerosol properties is possible over both water and land surfaces including regions that appear very bright in the IR. The values of the surface albedos are extracted from a climatological data-set derived from TOMS observations at 331, 340, 360 and 380 nm. Surfaces are assumed to be Lambertian and the values of surface albedo at 354 and 388 nm are obtained by interpolation of the TOMS climatology (National Aeronautics and Space Administration (NASA), 2007).

The footprint of the OMI observations is $13 \times 24 \text{ km}^2$ at nadir. Therefore the quality of aerosol products is significantly affected by cloud contamination. Currently the cloud mask used in OMAERUV is based on reflectivity thresholds, which can cause significant overestimation of the mean AOD. Previous experience with TOMS suggests that the algorithm is able to capture the variation monthly mean AOD. The AAOD is less affected by cloud contamination and hence is more reliable (National Aeronautics and Space Administration (NASA), 2007).

In general OMAERUV retrievals are more reliable over land than over water surfaces (National Aeronautics and Space Administration (NASA), 2007). The near-UV retrieval method is very sensitive to carbonaceous and mineral aerosols which are usually generated over the continents, and are characterised by high aerosol loads. On the other hand, dust and smoke aerosol events tend to take place under meteorological conditions which do not favour the formation of clouds in the vicinity of the sources. In case of sulphate aerosols the OMAERUV retrieved AOD is less accurate due to the low concentration, higher spatial variability and higher levels of cloud contamination.

Besides cloud contamination, ocean OMAERUV retrievals are affected by variations of surface reflectance. The spectral variations of ocean reflectance are accounted for by a climatological data set. Short-term variability cannot be taken into account in the current version of the algorithm and Ocean retrievals of AOD and AAOD sun glint angles smaller than 40° are not reported (National Aeronautics and Space Administration (NASA), 2007).

OMAERO

The OMAERO product is based on the so-called multi-wavelength aerosol retrieval algorithm based on the spectral information in the near UV and the visible between 342.5 nm and 483.5 nm. Including the near UV wavelength range allows the retrieval to distinguish between weakly absorbing and strongly absorbing aerosol types. Therefore, the OMAERO product can provide additional information on the aerosol type as compared to other aerosol products from sensors that do not include the near UV such as MODIS, MISR, or POLDER (Veihelmann et al., 2007). Current OMAERO data over land are not recommended for quantitative analyses because of possible errors due to the currently used surface albedo climatology. A reprocessing with improved surface albedo climatology was envisaged beginning of the year 2007 (Veihelmann et al., 2007), but is not yet available.

The multi-wavelength algorithm uses a set of aerosol models defined by size distribution, complex refractive index, and aerosol layer altitude. The models are representative for four major aerosol types including desert dust, biomass burning, volcanic and weakly absorbing aerosol. The particle shape is assumed to be spherical for all aerosol types, except for desert dust, for which the spheroidal shape approximation is used. The single-scattering properties of the dust aerosol models have been extracted from a pre-computed light scattering database, assuming the shape distribution that is used in AERONET retrievals for non-spherical aerosol types (Veihelmann et al., 2007).

The aerosol models are chosen in such a way to represent the most abundant aerosol types in the Earth's atmosphere. However the aerosol retrieval depends on the choice of the aerosol models. Look up tables of radiative properties of aerosols are used in the radiative transfer calculation.

In the case of OMAERO the surface reflection is taken from ocean model and land albedo climatology. In fact the surface reflection cannot be retrieved from OMI measured reflectance spectra independently from the aerosol parameters. Over oceans the reflectance of the surface is computed using a model that accounts for the chlorophyll concentration of the ocean water and the near-surface wind speed (Veihelmann et al., 2007). Over land the surface albedo spectrum is taken from a global seasonally resolved climatology assuming Lambertian reflectance at the surface (Veihelmann et al., 2007). In the latter case the surface albedo are based on the datasets of GOME, TOMS, MODIS or MISR (Veihelmann et al., 2007). Analyses of these surface data have shown that none of these datasets is optimal for usage in the multi-wavelength algorithm: currently, new surface albedo climatology is being generated that is derived from the three-year OMI dataset. It is expected that this new surface albedo climatology will improve the aerosol retrieval over land significantly (Veihelmann et al., 2007).

It is important to note that cloud contamination leads to an overestimation of the AOD and is considered to be one of the most important error sources.

Therefore OMI uses three tests to exclude cloudy scenes from the retrieval (Veihelmann et al., 2007):

- The first test excludes bright scenes with very low absorption using reflectance data in combination with the UV aerosol index (Veihelmann et al., 2007). Scenes with a reflectance larger than the threshold value of 0.3 and a UV aerosol index below 0.12 are classified as cloudy.
- The second test uses cloud fraction data from the OMI cloud product (OMCLDO2) and scenes with a cloud fraction larger than 0.34 are classified as cloudy.
- The third test is based on the spatial homogeneity of the scene. Inhomogeneous scenes with a small pixel variance larger than 0.00015 times the average radiance value are classified as cloudy.
- The last test results in the elimination of a large part of the cloudy scenes.

OMI also has an algorithm to exclude ocean scenes affected by specular reflection. Sun-glint screening can be performed using the sun-glint warning flag provided in the OMAERO product.

4.2.3 CALIPSO

A key piece of information that is not provided by most of the operating observational satellites is the altitude of aerosol layers in the atmosphere which is crucial information for studying the evolution of their distribution in the atmosphere. Indeed the aerosols confined to the lowest part of the atmosphere are likely to be removed quickly by rain while those that are transported to higher altitudes are much more likely to travel long distances and affect air quality in distant countries. Obtaining better information on the height of clouds is also needed. At present, weather prediction and climate models have considerable difficulty predicting the coverage, water and ice content and altitude of clouds. Inaccuracies in these parameters can lead to large errors in estimates of precipitation and the strength of the circulation. Observations from the Cloud-Aerosol Lidar and Infrared Pathfinder Satellite Observation (CALIPSO) provide both aerosol

and cloud height information that is valuable new information that will help to improve weather and climate forecasts.

The CALIPSO satellite provides a new insight into the role that clouds and atmospheric aerosols play in regulating Earth's weather, climate, and air quality.

CALIPSO combines three co-aligned, near nadir viewing instruments (Anselmo et al., 2007):

- A two-wavelengths polarization-sensitive lidar, CALIOP (Cloud Aerosol lidar with Orthogonal Polarization). The lidar provides information on the vertical distribution of aerosols and clouds, cloud particle phase and classification of aerosol size.
- An Imaging Infrared Radiometer (IIR) which provides medium spatial resolution nadir viewing images at 8.65, 10.6 and 12.05 μm providing information on cirrus cloud particle size and infrared emissivity.
- A high resolution wide-field camera (WFC) which collects daytime high spatial resolution images in the 620-270 nm wavelength range and is used to ascertain cloud homogeneity, to aid the cloud clearing process and to provide meteorological context.

CALIPSO was launched on April 28, 2006 with the cloud profiling radar system on the [CloudSat](#) satellite in a collaborative effort between the NASA Langley Research Center (LaRC), the Centre National d'Études Spatiales (CNES), Hampton University (HU), the Institut Pierre-Simon Laplace (IPSL), and Ball Aerospace and Technologies Corporation (BATC) to study global radiative effects of aerosols and clouds on climate (National Aeronautics and Space Administration (NASA), 2009).

CALIPSO and CloudSat fly in formation with three other satellites in the A-train constellation (including AQUA and AURA) to enable an even greater understanding of our climate system from the broad array of sensors on these spacecraft. Flying in the A-train constellation, CALIPSO offers, for the first time, the possibility of developing an integrated strategy between lidar and passive remote sensing techniques thanks to the synergies among different A-train sensors for both aerosols and clouds studies (Mona et al., submitted).

CALIOP, the lidar on board of CALIPSO, is an elastic lidar that provides vertical profiles of aerosol and clouds backscatter coefficients at 532 nm and 1064 nm and depolarization ratio profiles at 532 nm. Since the equation for a lidar in elastic configuration has two unknowns, the extinction and backscatter coefficients, an assumption on their ratio, i.e. the lidar ratio, is needed for retrieving profiles of extinction and backscatter coefficients from the CALIOP measurements. A first guess about lidar ratio is selected in CALIPSO retrieval algorithms on the type and subtype of the layer being analyzed and mainly on the base of AERONET climatological studies and model calculations (Mona et al., submitted). However, it has been observed that even for the same kind of aerosol, the lidar ratio can largely vary because of the natural variability of each aerosol species and of the aerosol modification/transportation processes (Mona et al., 2006, Müller et al., 2007, Müller et al., 2009, Papayannis et al., 2008). In order to validate the accuracy of aerosol optical properties retrieved from CALIPSO pure backscatter lidar, comparisons with ground-based elastic/Raman lidar measurements is necessary. This technique allows to measure vertical profiles of aerosol extinction and backscatter coefficients without any assumptions on the aerosol type and composition (Ansmann et al., 1992, Ansmann et al., 1990). However, before proceeding with the comparison on final CALIPSO products (namely the level 2 products), it is important to study and assess the accuracy of CALIPSO unprocessed (level 1) data (Mona et al., submitted).

CALIPSO produces level 1 and level 2 science data products. These products are archived and distributed by the Atmospheric Science Data Center (ASDC).

The level 1 data include (Hunt, accessed 2009):

- lidar calibrated and geolocated profiles for the day and night portions of the orbit, with associated browse imagery
- IIR geolocated, calibrated radiances registered to a 1 km grid centred on the lidar track
- WFC calibrated and geolocated radiance and bidirectional reflectance at 125 m and 1 km resolution for the daytime portion of each orbit. The 125 m resolution product covers the central 5 km portion of the swath.

Level 2 products include (Hunt, accessed 2009):

- cloud height, depth, backscatter, extinction, ice/water phase, emissivity, and ice particle size with horizontal resolutions of 1/3 km, 1 km and 5 km
- aerosol layer height, depth, optical depth, and integrated attenuated backscatter at 5 km resolution
- aerosol backscatter, extinction, and depolarization ratio profiles with a horizontal resolution of 40 km and vertical resolution of 120 m
- cloud with backscatter and extinction profiles and ice water content with a horizontal resolution of 5 km and a 60 m vertical resolution.
- a vertical feature mask with aerosol and cloud layer location (both vertically and horizontally), layer type, and the amount of horizontal averaging required for the layer to be detected
- IIR Level 2 cloud emissivity and particle size in 1 km pixels, with a 70 km swath width co-located to the lidar track

The main level 1 CALIPSO product that can be compared to Raman lidar data is the attenuated backscatter profile, defined as the range corrected lidar signal unless it is a constant (Hostetler et al., 2006). The attenuated backscatter profiles provided from CALIPSO data are not directly comparable to Raman lidar profiles, but a procedure has to be followed in order to compare PEARL and CALIPSO independent measurements. This procedure will be outlined in chapter 9.

Level 2 Profile data contain the vertical profiles of the following quantities that can be compared to the Raman lidar directly:

- total backscatter coefficient at 532 nm
- perpendicular backscatter coefficient at 532 nm
- backscatter coefficient at 1064 nm
- particle depolarization ratio at 532 nm
- extinction coefficient at 532 nm
- extinction coefficient at 1064 nm

In the level 2 data CALIPSO also provides layer integrated quantities for each identified aerosol layer, such as integrated attenuated backscattering at 532 and 1064 nm, integrated colour ratio and integrated volume depolarization ratio.

4.3 Validation approach

4.3.1 *Strategies for validation of ozone and temperature profiles derived from satellite measurements*

The validation approach used in this project has been outlined in 'EQUAL Annual Report 2004' (Meijer et al., 2005b), which as a final result provides comparisons of ground- or balloon-based measurements with profiles retrieved by satellite instruments. This comparison comprises lists of collocations with pointers to the measurements and a range of comparison images grouped on specific measurement conditions (for instance star magnitude). The validation approach and target level-2 data quality have also been described in Meijer et al. (2004, , 2005a).

4.3.2 *Strategies for validation of cloud and aerosol products from satellite measurements*

As stated before, one of the reasons for the great uncertainty on the role that aerosol and clouds play on climate is their high variability in time and space (Forster et al., 2007). Studies involving the monitoring of aerosol load during long periods of time can help understand their natural seasonal variability and their variations in the presence of special large scale events (volcanic eruptions, large forest fires etc.). The study of the variation of the aerosol optical depth both from satellite and from a ground based instrument, like the Raman lidar, can help define the spatial scale of this variability.

Based on the amount of Raman lidar data available and on the kind of satellite products available, we identified two types of strategies for performing satellite validation:

- One strategy is to compare quantities in a climatological or statistical sense, which means to perform comparisons on a dataset that spans years of measurements. This kind of validation does not require strictly collocated measurements and allows studying the average correlation between satellite and ground based measurements. This is the strategy that can be used for studying the aerosol optical depth measurements from satellites like MODIS and OMI, for example.
- The other strategy is a point to point validation and requires correlative measurements with the lidar to the overpass of the satellite. This strategy allows a more detailed comparison of the satellite measurements and is the strategy used within EARLINET for the validation of CALIPSO. In particular in the case of CALIPSO the validation allows to compare vertically resolved features within a single profile, for which the time and space correlation is a key requirement.

In chapters 8 and 9 we present examples of both climatological validation of an aerosol optical depth dataset collected by MODIS and point to point validation of CALIPSO profiles focusing on the use of the CNR-IMAA Raman lidar.

At CNR-IMAA, an elastic/Raman lidar for aerosol study has been operating since May 2000. In its first configuration, PEARL (Potenza EARlinet Lidar) provided: simultaneous and independent measurements of aerosol backscatter and extinction at 355 nm, aerosol backscatter coefficient at 532 nm with an assumption on the lidar ratio, and vertical profile of the water vapour mixing ratio. PEARL was operational with this configuration for more than 5 years, until August 2005, when we the system upgrade started. Since May 2006, PEARL is a multi-wavelength Raman lidar capable of retrieving the aerosol backscatter coefficient at three wavelengths (355, 532 and 1064 nm) and the aerosol extinction coefficient at two wavelengths (355 and 532 nm), and in addition the water vapour mixing ratio and depolarization ratio profiles at 532 nm.

Since the beginning of EARLINET in 2000, lidar measurements are regularly performed at the CNR-IMAA three times per week following the EARLINET measurements schedule described in section 2.1.3. Moreover additional measurements are specifically performed to investigate particular events of aerosol transport (Amodeo et al., 2007).

The CNR-IMAA lidar station has been involved with EARLINET since the beginning of the project in 2000. Since then it has been collecting a large amount of Raman lidar data, both during regular measurements and in presence of events such as Saharan dust transport and volcanic eruptions (Amodeo et al., 2007). The station is located at (40°36'N, 15°44' E) at an elevation of 760 m which makes this site particularly interesting from the point of view of the study of aerosols. The typical aerosol that can be sampled at CNR-IMAA is a mixture of marine aerosols (the station is located at around 100 km from the Tyrrhenian, the Adriatic and the Ionic sea) and

continental aerosols. Because of its location, the CNR-IMAA station is also very often capturing Saharan dust transport events. These characteristics make the CNR-IMAA station an interesting laboratory for the study of the optical properties of different types of aerosols and clouds.

4.3.3 *Software development*

The validation software has been extended to deal with SCIAMACHY data from IUP Bremen (Stratozone and intermediate products for verification purposes) and MIPAS data from Oxford University. Preparations have also been made to ingest OMI level 2 data, but this has not yet been thoroughly tested. In addition, the produced comparison images have been updated on feedback from the GOMOS quality working group and the NDACC lidar working group. We now also compute standard errors and percentiles.

The EARLINET data provided within the VALID project will have to be stored in the CALVAL ESA database. For this reason they will have to be converted from the EARLINET netCDF format to the ESA HDF format. A Java tool has been provided by NILU to convert ASCII files into the desired HDF format. A NetCDF to ASCII converter has been developed by CNR-IMAA and can be used to generate properly formatted files for to the ASCII to HDF converter. During the work performed for VALID some example EARLINET files containing both backscattering and extinction coefficient profiles have been converted to HDF. At present the conversion has to be done manually and for a single file at a time, since the information about the stations has to be selected from a precompiled list. In the coming year we will work on automating this process so that large numbers of files can be converted simultaneously, which will be necessary as the number of files to be submitted to the ESA database is expected to increase in number.

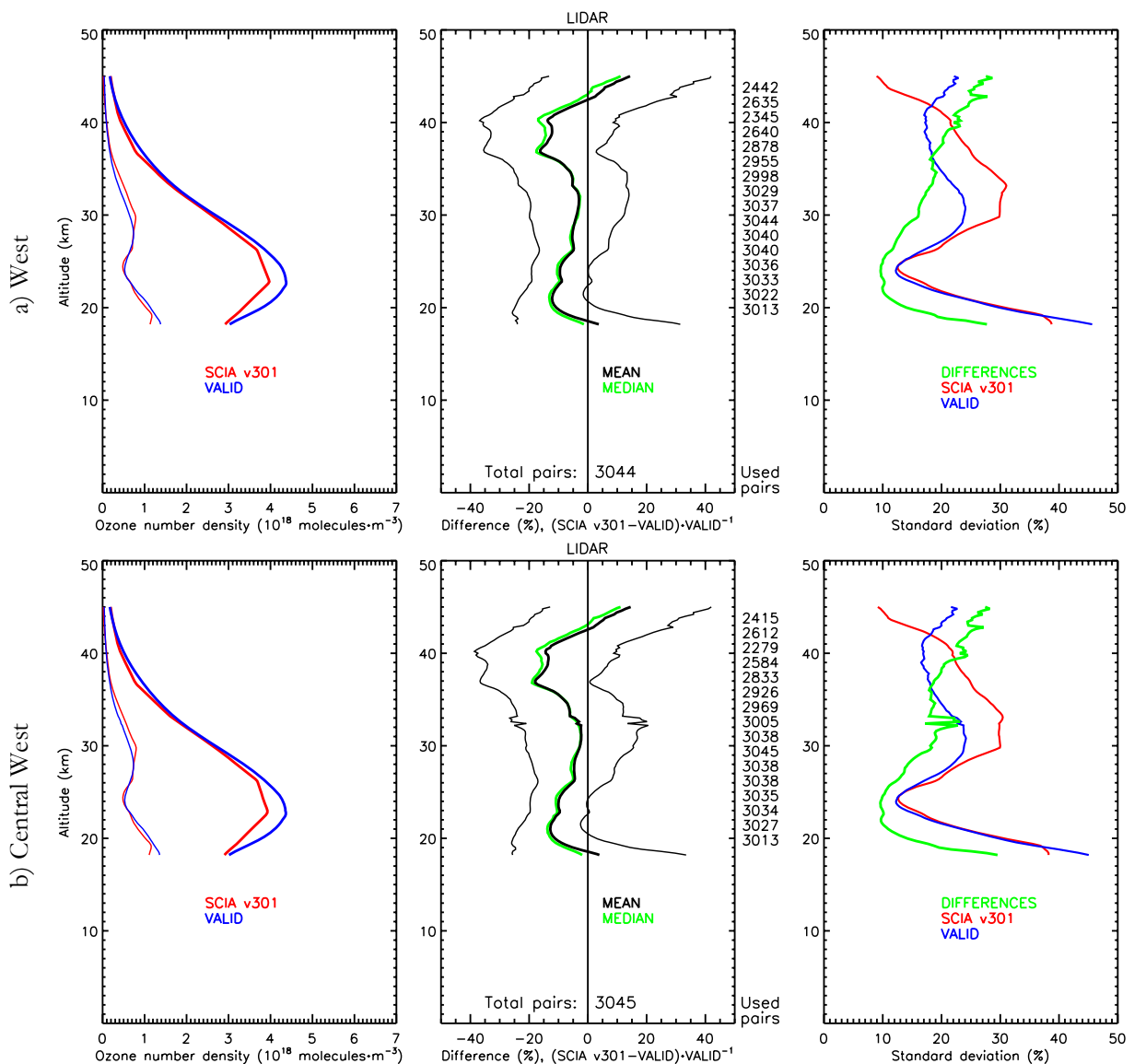
The following three chapters will provide an overview of the validation results obtained per atmospheric instrument onboard ENVISAT during 2008. After that, two chapters will present examples of climatological validation of an aerosol optical depth dataset collected by MODIS and point to point validation of CALIPSO profiles.

5 SCIAMACHY

Temperature profiles in the SCIAMACHY files are climatological values and they are not retrieved. Originally it was foreseen to retrieve temperature information from the infrared channels, but these measurements suffer from ice on the detectors, which makes it impossible to retrieve temperature. The current status for alternative algorithms using measurements from the other channels is unclear for the operational processor.

Ozone profiles from the operational processor IPF version 3.01 show a reasonable agreement with the lidar data. There is a negative bias of 0–15% in the altitude range 18–40 km. Above 40 km, no actual retrieval is performed and reported values are climatology. Comparisons in the altitude range 18–38 km show that the precision of SCIAMACHY is better than 10–15%. Similar to version 3.00, the high ozone concentrations in the ozone peak and the profile just below the peak are underestimated by about 10–20% in all regions.

In Figure 5 we show validation results of these SCIAMACHY ozone profiles for the years 2002–2007 compared to lidar data. The dataset has been grouped into the different limb scans (West, central West, central East, East or unknown). Differences between the distinct scan positions are very minor (Figure 5a-d), except for the profiles that were tagged to have an unknown position (Figure 5e). This last case only occurs close to the Polar Regions (above 62.9°N for the collocated data used here), hence the particular shape of the average ozone profile.



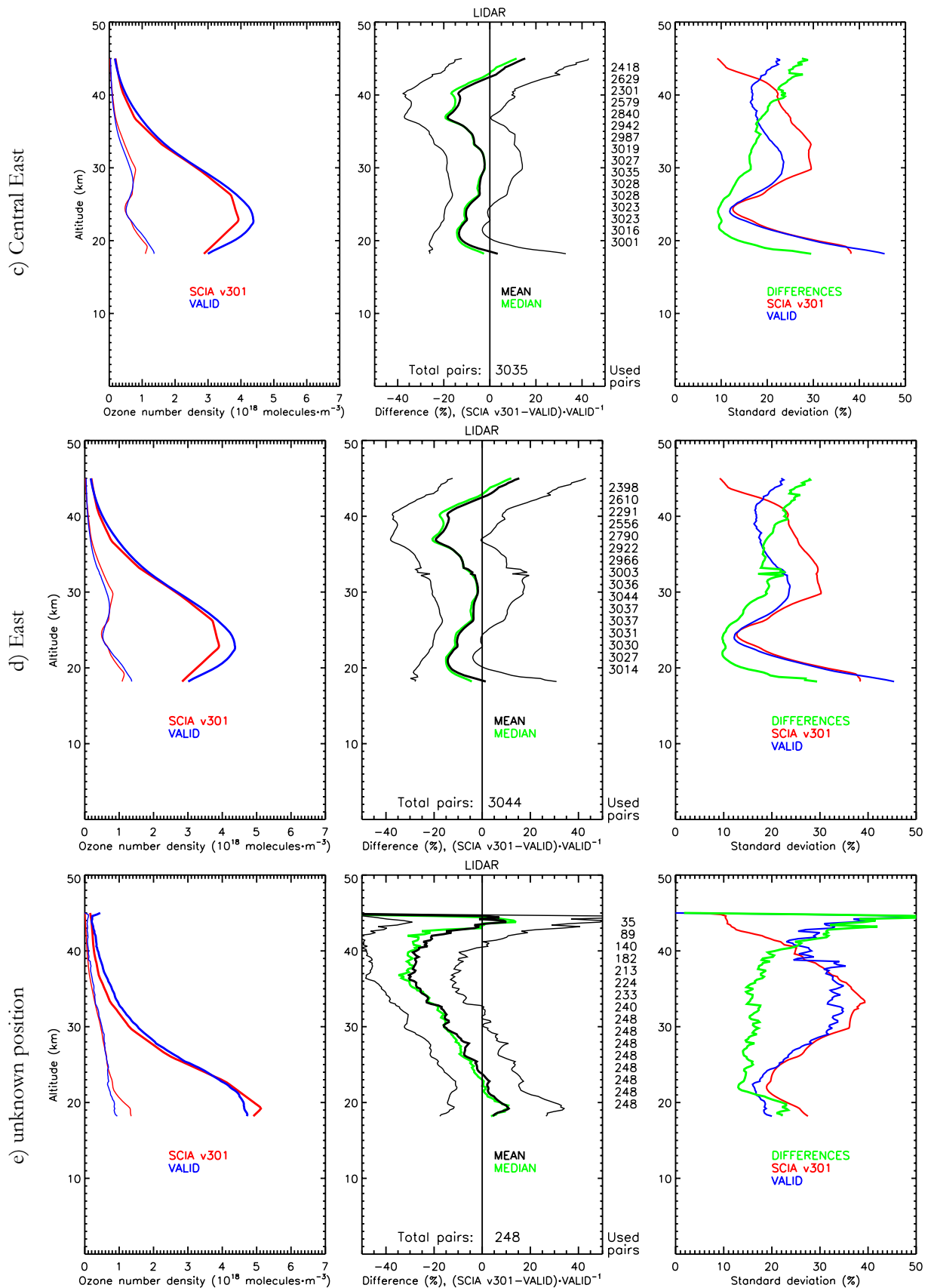
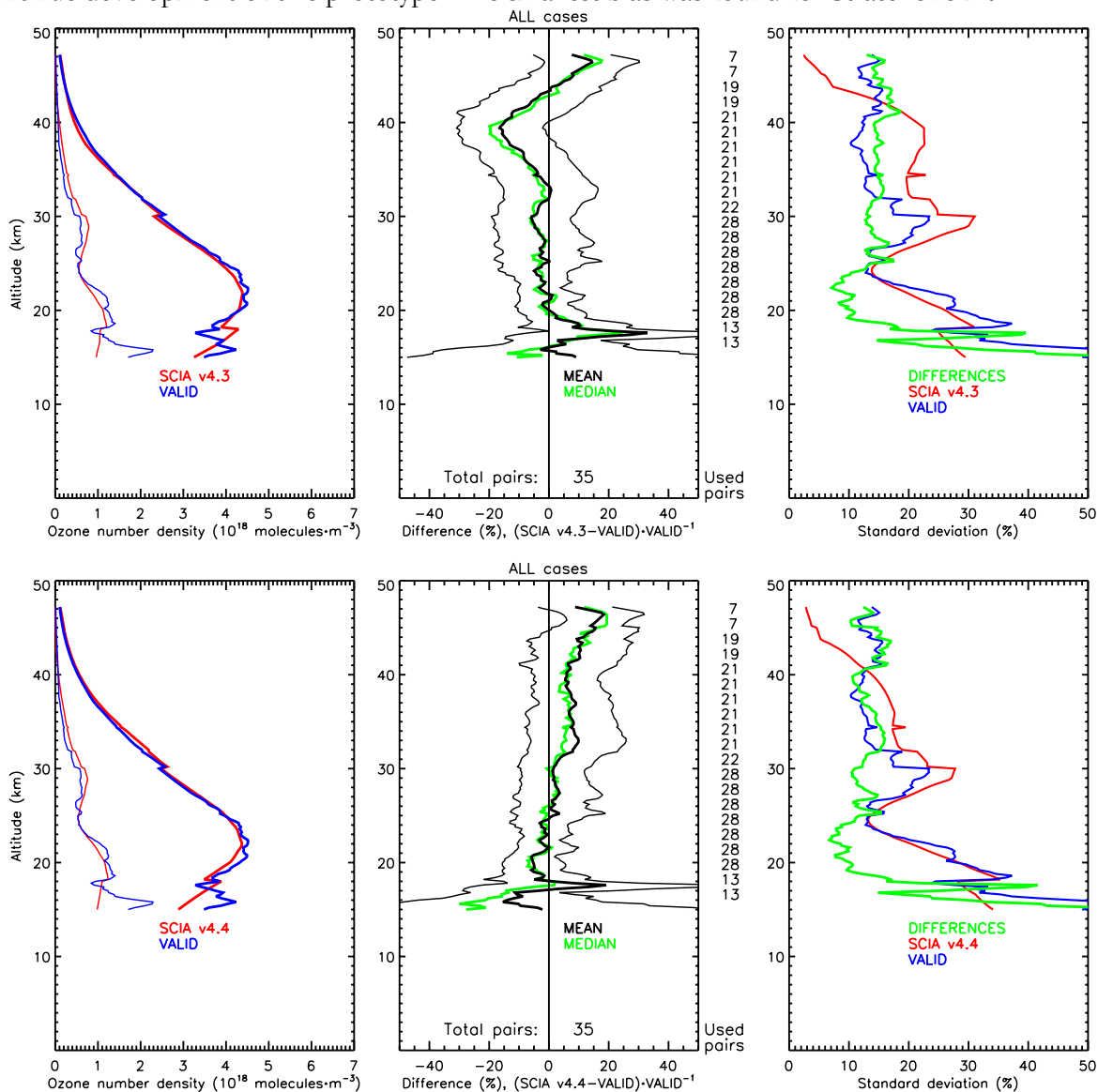


Figure 5: SCIAMACHY ozone profiles retrieved with IPF 3.01 compared with lidar measurements for the four limb scan positions: a) West (-2); b) Central West (-1); c) Central East; (1) d) East (2); e) no data available on scan position.

Left panels show average SCIAMACHY (thick red line) and ground-based (“VALID” thick blue line) with their respective standard deviations (thin lines) as a function of altitude. The middle panel shows the median (green) and the mean (black) difference between SCIAMACHY and

VALID plus minus one standard deviation (thin black lines). On the right of this panel is the number of collocating pairs as a function of altitude. Right panels show the standard deviations of SCIAMACHY (red), VALID (blue) and the individual differences (green)

In 2008 we also carried out a verification for version 4. A small verification dataset run with the two candidate algorithms (referred to as 4.3 and 4.4) were compared with version 3.01 and with scientific algorithms from IUP Bremen. In the validation dataset we used sonde, microwave radiometer and lidar data. Out of the two candidate versions, version 4.4 was chosen to match the ground-/balloon-based measurements most closely and thus it was recommended to continue development of this prototype. The smallest bias was found for Stratozone 2.0.



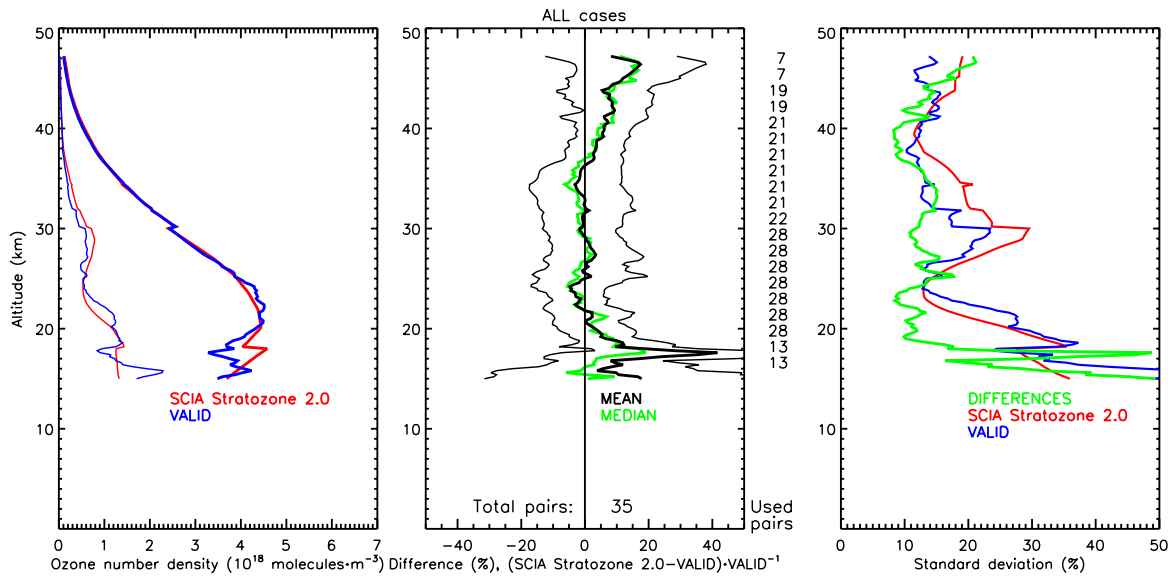


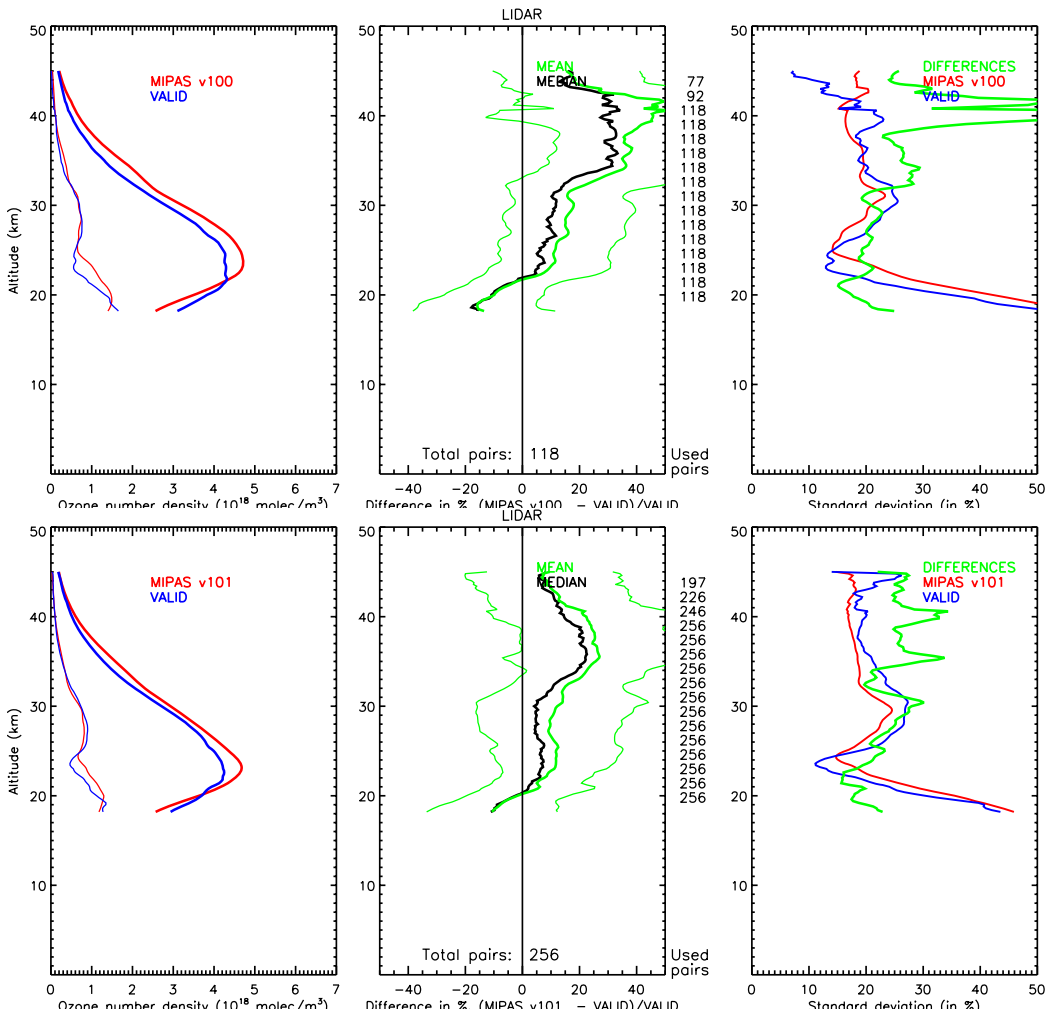
Figure 6: as Figure 5. now showing the verification results for SCIAMACHY test versions 4.3 (top) and 4.4 (middle) and Stratozone 2.0 (bottom)

Additionally, in 2008 we started validation of the full SCIAMACHY time series processed with Stratozone 2.0. This version contains a cloud flag and averaging kernels are produced with each processed profile. The validation was not fully completed as a result of communication delays. As the SCIAMACHY dataset is rather large, we seek to re-run the analysis on a more powerful processing unit in 2009.

6 MIPAS

In 2008, no data from operational ESA processor was available, as the implementation of changes from version 4 to 5 turned out to be far more complicated than initially foreseen. Nevertheless we worked on the identification of a new extended validation dataset. To do so, all level 1 data from 2002 to the beginning of 2008 was downloaded and latitude, longitude and time of measurements were extracted. This information was also provided to the TASTE team, so that they could assemble an additional collocation set for specific instruments. The information from the level 1 data was subsequently matched against all profiles in the validation database to filter the candidates based on given collocation criteria. Various lists were created this way (one for ozone, one for temperature and one reduced set which corresponded to all occurrences that were also in the TASTE lists).

Since no operational data was available for validation, we decided to examine the scientific algorithms. In 2008 we prepared all scripts to ingest profiles prepared by Oxford University's MORSE algorithm. Data from three versions covering parts of June 2007 to January 2008 were tested. Unfortunately, the data processed with the distinct versions do not overlap and direct comparison was thus not possible. Figure 7 shows the comparison with lidar data for the three versions. Note that no averaging kernel has been applied to the lidar profiles. It is clear that progress is made with the sequential versions where for version 1.02 the ozone profiles match up very well to the lidar profiles until an altitude of 30 km. Above this altitude, the algorithm starts to overestimate the ozone concentration to reach a maximum overestimation around 40 km where the median deviation is about 20%. Also we see some outliers around this altitude (mean \neq median).



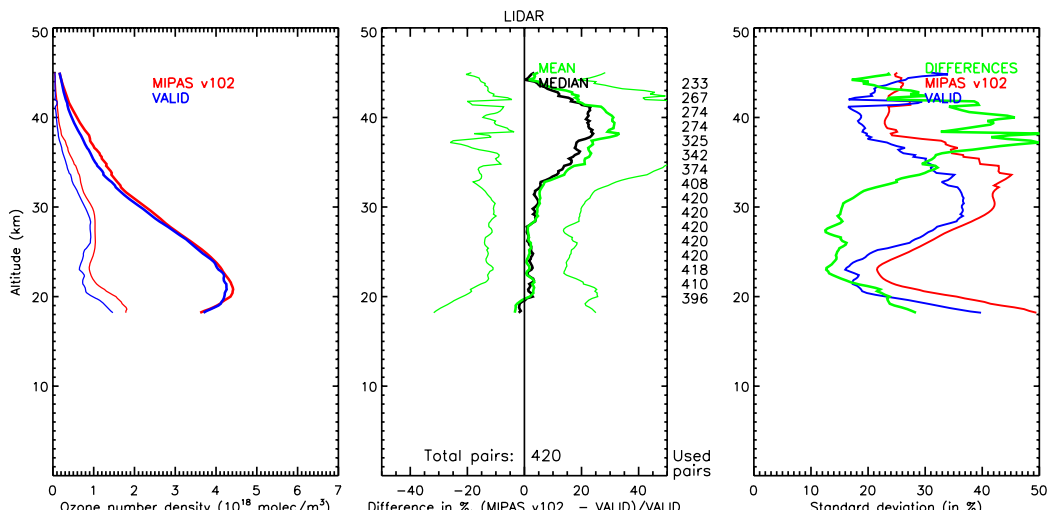


Figure 7: Same as Figure 5 but with colours for mean and median swapped; showing results of MIPAS ozone profiles for MORSE versions 1.00 (top), 1.01 (middle) and 1.02 (bottom) profiles compared to lidar data.

Note that the subplots correspond to different datasets and can therefore not be compared directly.

Figure 8 shows the comparison for version 1.02 temperature profiles with sonde, microwave and lidar data. A peculiar kink is seen around 30 km, but for most of the profile, data is within 1 Kelvin. In 2009 we hope to have a look at a larger dataset spanning a longer time series.

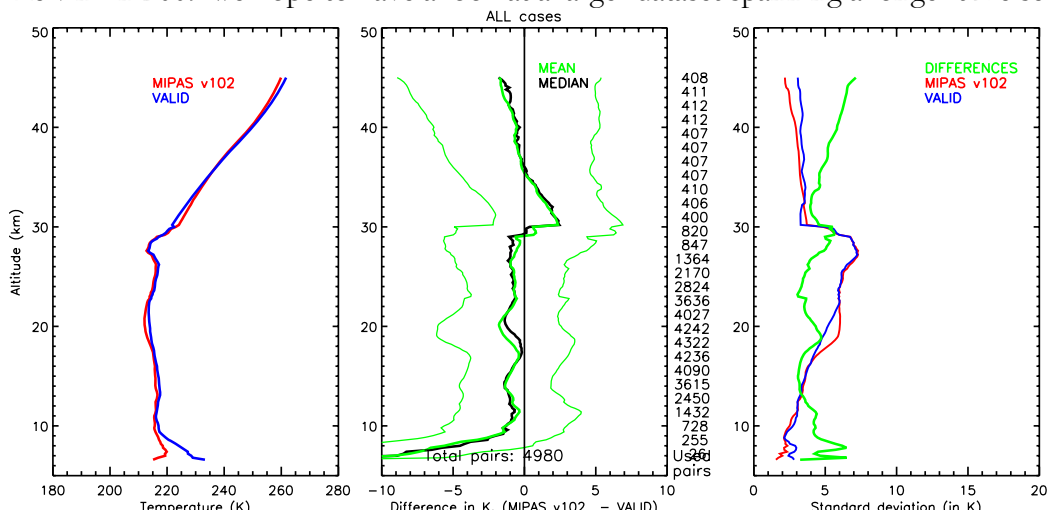


Figure 8: Same as before, now showing comparison with MIPAS temperature profiles for MORSE 1.02 compared to sonde, lidar and microwave data

Note that the scale used for the temperature comparison is absolute rather than relative (middle and right bottom panels), and that the altitude range is more extended. The altitude information for the MIPAS profiles has been obtained by transferring MIPAS pressure data to geometric altitude using ECMWF data interpolated to the position of the MIPAS profile.

7 GOMOS

GOMOS ozone profiles (IPF 5.00) have shown an excellent agreement with lidar data with a bias within 5% between altitudes of 15–45 km.

Some discrepancies were previously found in the Polar Regions (Meijer et al., 2004, van Gijssels et al., 2008). Although these measurements were performed at solar zenith angles of greater than 108° , the processor has assigned flags for twilight and/or straylight contamination (see <http://envisat.esa.int/handbooks/gomos/CNTR3-3.htm> for the criteria). No collocations with lidar profiles are found in Polar Regions with so-called dark profiles (see Figure 10 and (Guirlet, 2009)), although some collocations with sonde measurements exist (Figure 9). Most collocations occur with the Dumont d'Urville sonde. For this particular station, we find various large outliers in the differences. This phenomenon will be further studied, paying attention to the respective locations of the sonde and GOMOS measurements given the position of the vortex.

Disregarding the Dumont d'Urville measurements reduces the number of available correlative points substantially, yet only two stations give collocations with dark limb measurements.

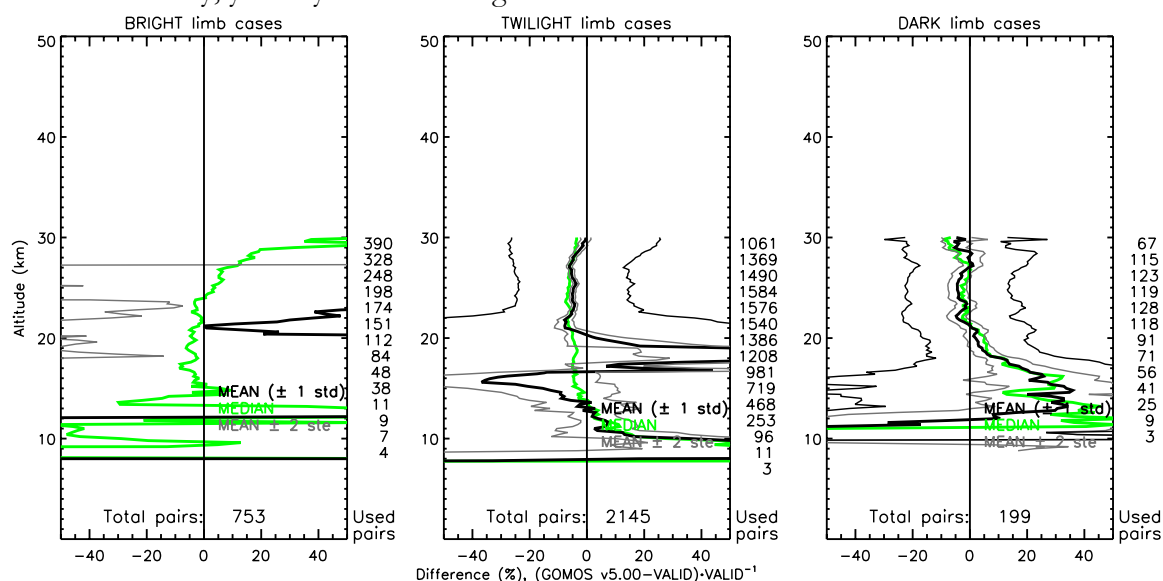


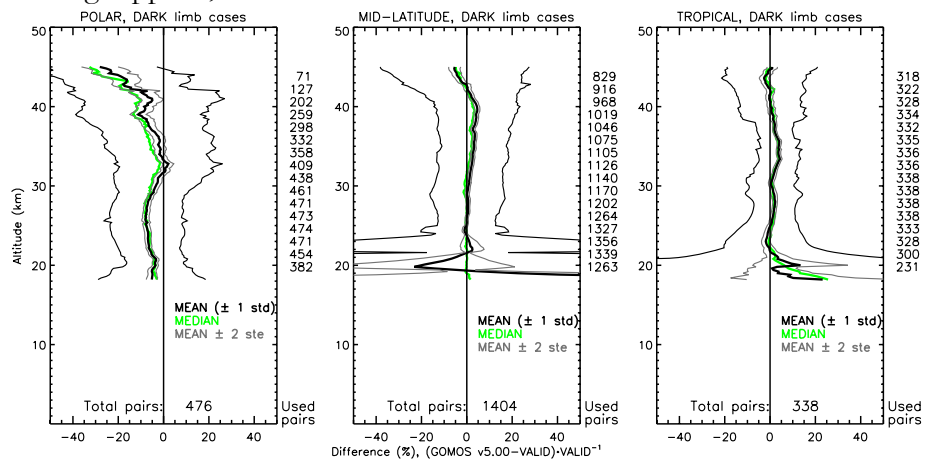
Figure 9: Results for collocation with polar sondes where all GOMOS measurements were taken above 66.5° latitude. Left panel: bright limb cases; middle panel: twilight limb cases; right panel: dark limb cases. On the x-axis is the difference in percentage, y-axis covers the altitude range from 0 to 50 km. The green lines indicate the median difference profile, thick black lines the mean differences (plus/minus one standard deviation as thin black lines and plus/minus two standard errors as thin grey lines). On the right of each panel is the number of used collocation pairs for a given altitude.

From Figure 10 it becomes clear that application of the limb flag does not sufficiently remove all outliers in the mid-latitude region.

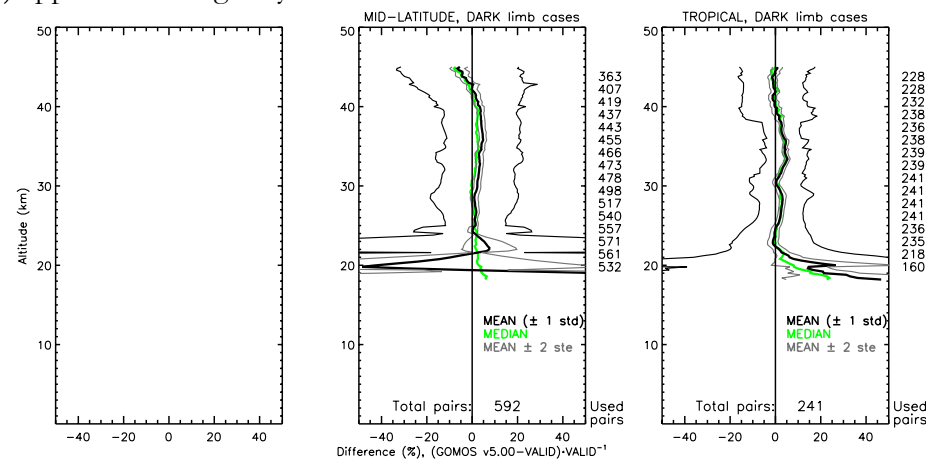
It is questionable if all profiles measured in the Polar Regions should be removed as is done when applying the limb flag. When considering only the species flag (Figure 10c), the pattern is very similar to when only a filter is applied based on the solar zenith angle and no particular differences can be pointed out for this region. Nevertheless, the significant bias observed between 20 and 30 km cannot be backed up by the few (87 to 128) full-dark limb cases collocating with sonde measurements (Figure 9), where the mean deviation is showing a negative bias, but this is mostly not outside the two standard errors region and thus not significant. However, when looking at the two sites individually, the bias is visible at Marambio (5 to 10% underestimation by GOMOS), not at Belgrano (which shows an overestimation of about 7%). In addition, all comparisons with lidar are for the Northern Polar Region, whereas those with the sondes in dark are all in the Southern Polar Region.

More detailed analyses should be carried out considering the vortex position and the differences between the two hemispheres.

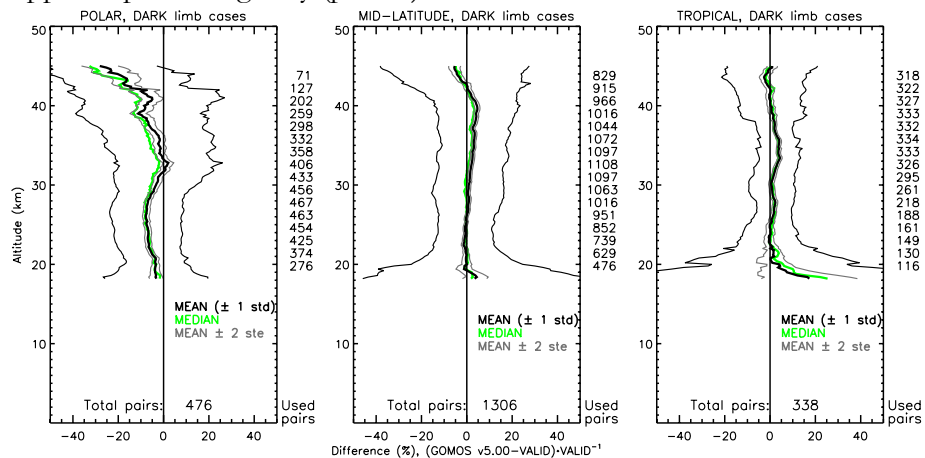
a) no flags applied, dark = $\text{SZA} > 108^\circ$



b) applied limb flag only



c) applied species flag only ($\text{pcd}=0$)



d) applied limb flag and species flag

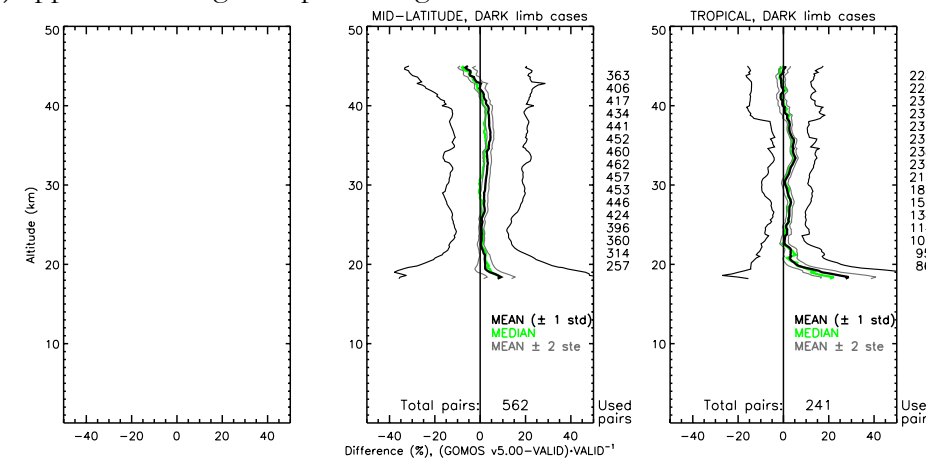
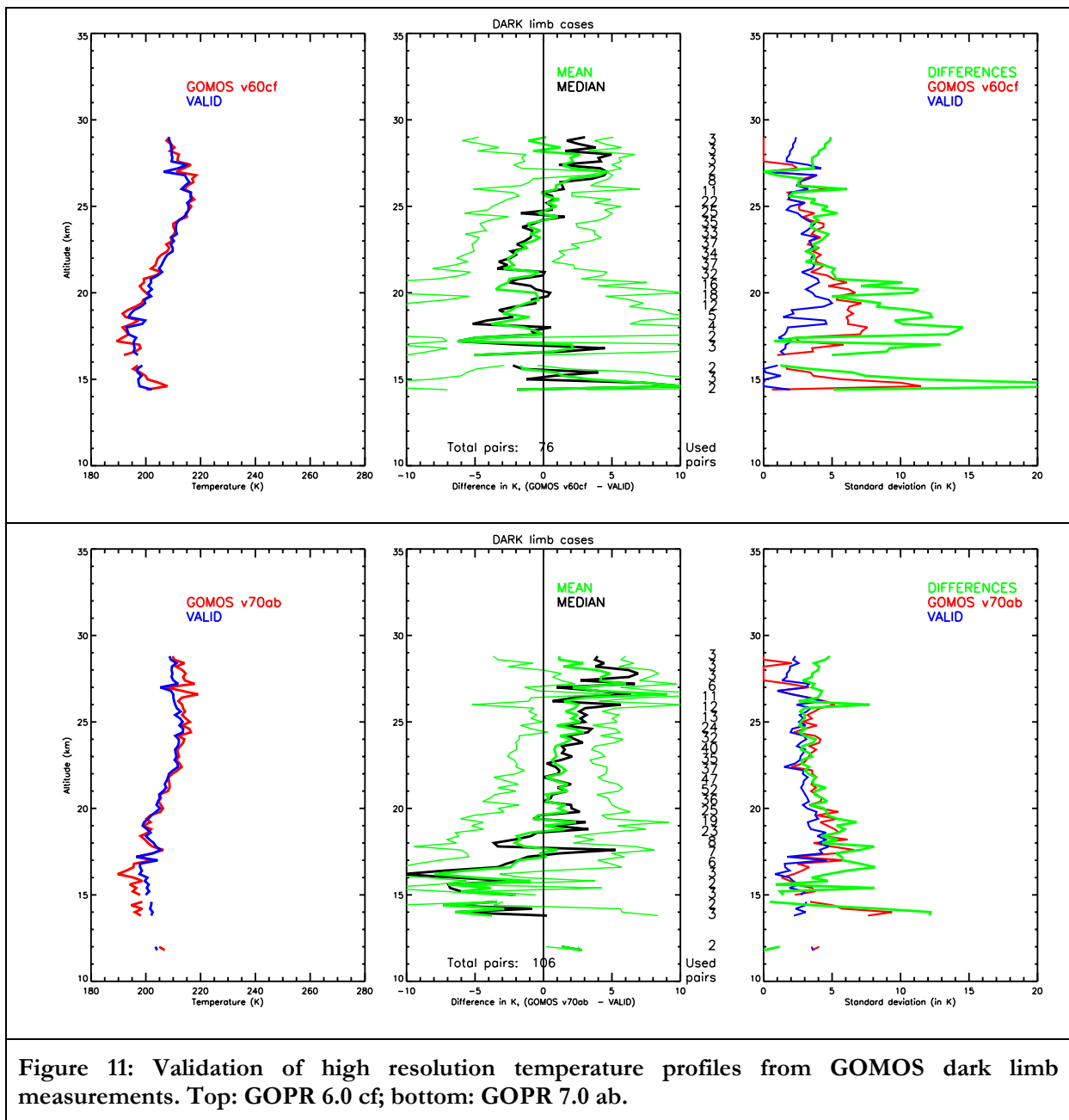


Figure 10: Validation results for GOMOS IPF 5.00 compared to lidar data considering different flags for the three main geographical regions (left panel: polar regions; middle panel: mid-latitudes; right panel: tropics). Top left (a): cases where the solar zenith angle (SZA) is greater than 108 degrees, flags are not considered; top right panel (b): same dataset now considering the flag indicating the limb condition assigned during processing; bottom left panel (c) same dataset disregarding the limb flag, but considering the validity flag for the measured species; bottom right panel (d) same dataset considering both the species and the limb flag.

Comparing GOPR 6.0cf with GOPR 7.0ab, we found that hardly any differences were visible in the ozone profiles. Version 7.0ab appears to have fewer outlier ozone profiles, but since the definition of the reported error has changed, it could also be that profiles corresponding to outliers in version 6.0cf had been rejected if they exceeded the maximum error allowed (30%). It was also suggested at the GOMOS QWG#18 that most outlier profiles can be removed by applying a minimum (0) and maximum (10^{19} molecules/m³) ozone concentration filter. The Quality Working Group did not support this approach as they did not want to introduce a-priori restrictions which could lead to biases.

Version 7.0ab for the high resolution temperature profiles (HRTP) hinted at an improvement compared to version 6.0cf, but still substantial deviations are found (Figure 11). Nevertheless, the available HRPT dataset is very limited (most profiles are not containing any data). Further development of the algorithm is thus recommended.



8 MODIS

In this section 5 years of AOD measurements obtained with PEARL have been compared to the measurements of AOD obtained with MODIS-Terra at 550 nm (Mona et al., 2008). A total of 140 Raman lidar measurements of night time aerosol extinction profiles were available from May 2000 to April 2005 at 355 nm. The aerosol optical depth has been calculated integrating the entire Raman lidar profile. A total of 2800 daytime AOD measurements were available from MODIS from May 2000 to January 2008.

Figure 12 shows the AOD measurements at 355 nm at CNR-IMAA integrated over the whole column (panel a), together with the percentage contribution of the free troposphere to the aerosol columnar load (panel b). The free troposphere (FT) contribution is calculated starting from the Planetary Boundary Layer (PBL) top height, which represents the layer closest to the surface where most of the aerosol content is usually confined. The FT contribution, as defined in EARLINET, is the fraction of AOD above the PBL with respect to the total AOD, expressed in percentage. This quantity helps to separate between cases in which the aerosol is confined in the PBL (low FT contribution) and cases in which there is significant aerosol load in the free troposphere (high FT contribution). This parameter also helps to identify large scale processes, which are characterized by a high FT contribution. The PBL is retrieved, according to EARLINET definition, as the first minimum of the backscattered range-corrected lidar signal (Matthias et al., 2004).

In Figure 12 (panel a) a seasonal cycle in the AOD is clearly evident. Over five years of measurements a mean total AOD of 0.4 is obtained, but a decreasing trend is evident. In particular, the highest values (around 0.7) are on average observed during spring-summer 2000, while during the same seasons in the following years lower values are observed. In addition, during the period May 2004 – April 2005, a smaller difference between AOD measured in warm and cold seasons is observed. During this last year, in fact, cold seasons were characterized by a higher AOD if compared to the same period of the other years, while the values measured in the warm seasons are lower than in the previous 4-years. The FT contribution suggests that this behaviour is related a prevailing contribution of the aerosol in the free troposphere during Autumn-Winter 2004-2005 with respect to the other years, when the FT contribution typically stays lower than 30%.

Figure 13 shows the temporal variation of the aerosol optical depth measured by MODIS at 550 nm ($1^\circ \times 1^\circ$ resolution for collection 5) from May 2000 to January 2008 in a region centred on Potenza. As in Figure 12, a difference in the annual behaviour of AOD in 2004-beginning of 2005 is evident. MODIS data in fact confirm that during this year the variation of the AOD observed during winter and summer is smaller than during the other years. In addition, MODIS measurements allow ascribing this phenomenon to large scale processes not confined in the area of Potenza. A more quantitative comparison between PEARL and MODIS measurements is possible by scaling the MODIS data at 550 nm to 355 nm with the mean Ångstrom exponent measured with the AERONET station located at CNR-IMAA. MODIS measurements are performed during the day while lidar measurements are performed mostly during the night and the assumption that the difference in time is not significant for a dataset including years of measurements has to be made.

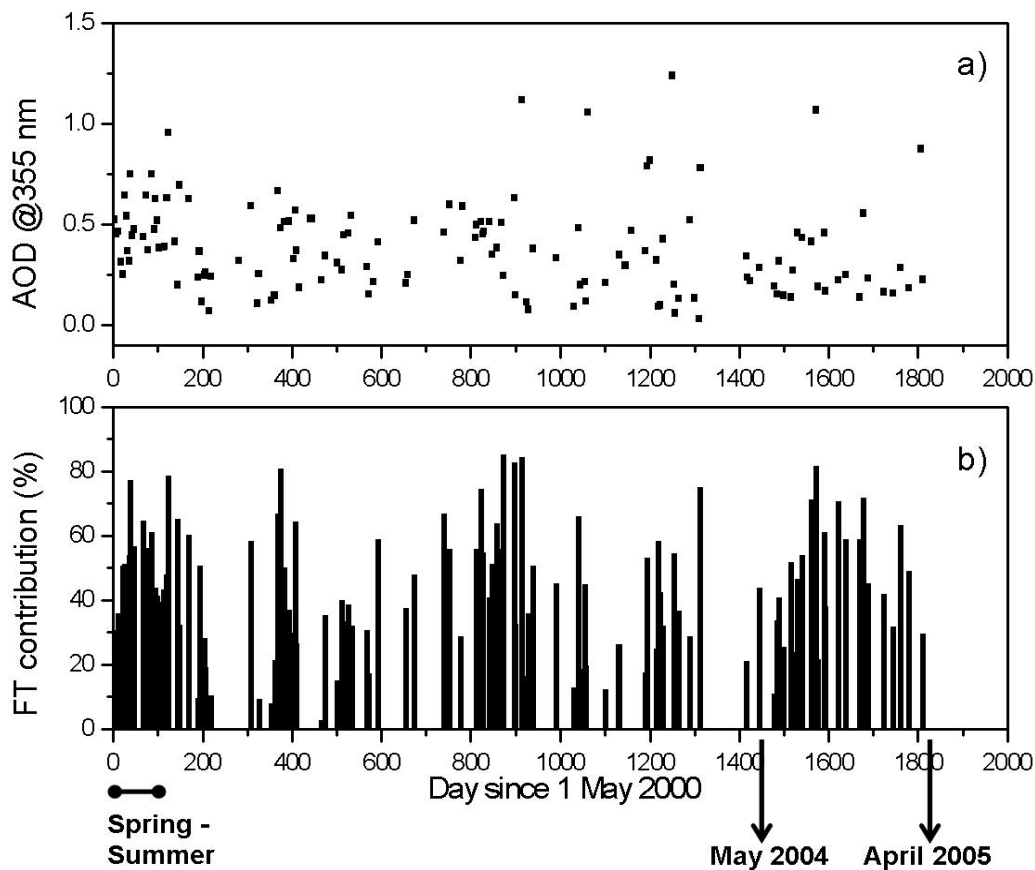


Figure 12: AOD measured at 355 nm by PEARL since May 2000 (panel a) and FT contribution to the total aerosol AOD (panel b)

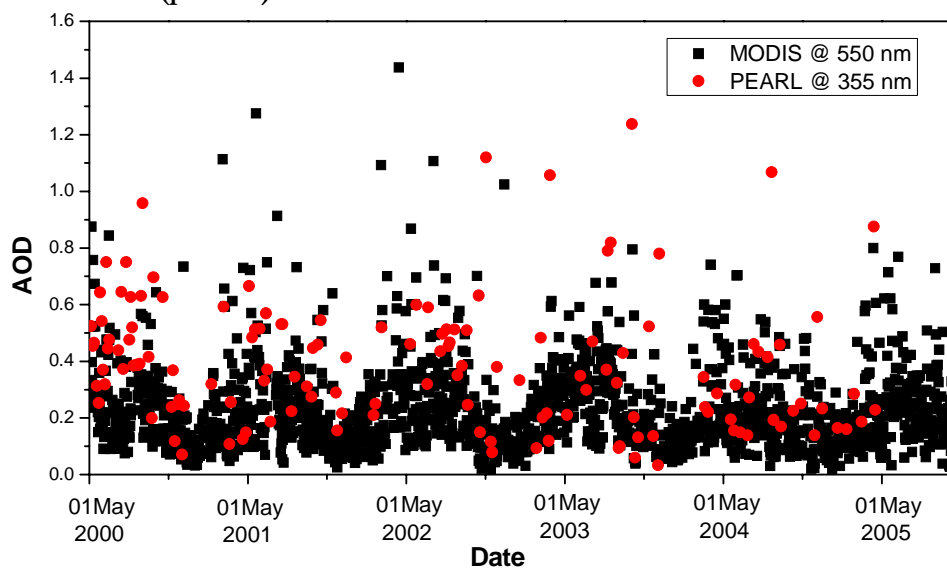


Figure 13: AOD measurements at 550 nm by MODIS in a 1 degree \times 1 degree area centred on Potenza. The MODIS AOD data are displayed together with the PEARL data already shown in Figure 12. The MODIS data used here are MOD08_D3, which are extracted from MODIS level 3 low resolution daily images collected from Terra MODIS.

Therefore this comparison allows only to obtain mean information and to highlight the main interesting and critical points in the active ground-based versus passive satellite measurements comparison. However the possibility of increasing the number of lidar measurements by adding data from other EARLINET stations increases the possibility to derive increasingly specific information on the aerosol distribution and evolution. In this comparison a mean Ångström exponent of 1.3 was calculated from the AERONET measurements and a very good agreement

is found between PEARL and MODIS scaled AOD with a mean difference of 0.002 ± 0.16 . Nevertheless, the individual absolute differences range between 0.0005 and 0.87. In order to investigate high difference values, the capability of lidar to provide vertical profiles is used. Therefore we separated the dataset in two groups based on the values of FT contribution using as a threshold value of 30 %.

Figure 14 (panel a) shows the difference in AOD measured by PEARL and MODIS as a function of the FT contribution to the total columnar aerosol load. It is clear that even if on average the two measurements are in agreement, the largest differences are observed in the cases of high aerosol load in the FT. Figure 14 (panel b and c) reports also the probability distribution function of the PEARL-MODIS differences in the two classes defined by the FT contribution. Both distributions are well fitted by a Gaussian distribution with a mean value around 0, but the standard deviation of the fitting curve for cases with high FT aerosol load is almost double with respect to the other class (0.20 compared to 0.13). Therefore we can conclude that in the presence of lofted aerosol up to the FT, which typically indicates large scale processes, differences between satellites $1^\circ \times 1^\circ$ measurements and punctual measurements of the AOD can be as high as about 100 % (Mona et al., 2008).

Outlook

In the next years similar climatological validation studies will be performed. Since 2005, aerosol extinction profiles from PEARL are also available at 532 nm and they are more suitable for this kind of validation since they are closer in wavelength to the MODIS wavelength. Similar validations will be performed using also OMI aerosol optical depth measurements. Initially these studies will be performed using data from the CNR-IMAA station, and then this activity will be extended to other EARLINET stations. For this activity the EARLINET data used in the comparisons will not be duplicated at the ESA CAL/VAL database at NILU.

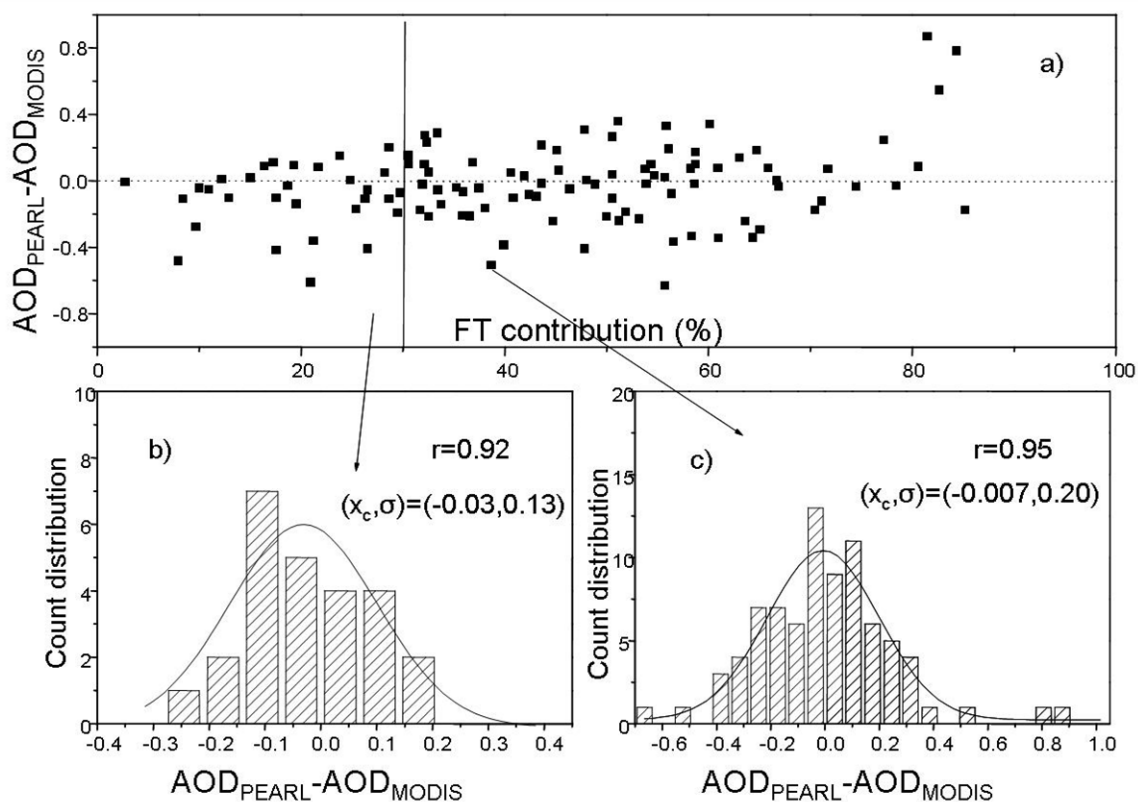


Figure 14: Differences between PEARL and MODIS measurements of AOD as a function of the FT contribution to the total aerosol load (panel a). Data are divided into two classes related to the FT contribution lower and higher than 30%. Histograms of the observed differences are reported for the two classes (panel b and c).

9 CALIPSO

Here we report on the recent activity performed at the CNR-IMAA on the validation of CALIPSO aerosol profiles with the Raman lidar PEARL. The validation of CALIPSO profile products is of great importance to the CALIPSO mission and to ESA, since the validation strategy defined for CALIPSO will be applied also to the validation of ESA satellite products. As outlined in section 4.2.3, CALIPSO hosts a backscatter lidar which collects the radiation that is elastically backscattered by the atmosphere. In order to retrieve backscattering and extinction coefficient profiles from this instrument it is necessary to make assumptions on the value of their ratio, called the lidar ratio. Within CALIPSO this assumption is made considering an extended lidar ratio climatology which reports the most commonly measured lidar ratios for different kinds of aerosols. A Raman lidar can directly measure that quantity without any assumption on the type of aerosol. For this reason the validation of the profiles of aerosol optical properties retrieved by CALIPSO using Raman lidar measurements, can help validate the assumptions made by CALIPSO on the lidar ratio. Moreover the comparisons of the level 1 data can help verify that the lidar onboard CALIPSO is operating properly.

As stated previously, since May 2006, CALIPSO is providing high vertical resolution aerosol profiles. In order to increase and validate the accuracy of aerosol optical properties retrieved from CALIPSO pure backscatter lidar, comparisons with ground-based lidar as reference points is strongly necessary. Ground-based lidar measurements at 3+2 wavelengths are an optimal tool for validation of CALIPSO products, because they provide independent measurements of the particles backscatter and extinction at 532 nm and backscatter at 1064 nm profiles that can be directly compared to analogous quantities derived from CALIPSO. However, before these comparisons, it is essential to investigate the CALIPSO raw signal to identify possible biases. Only after a check of the unprocessed CALIPSO data, the comparison in terms of level 2 products will allow to check and improve CALIPSO retrieval algorithms and assumptions. Comparing first ground-based versus CALIPSO level 1 allows distinguishing problems and biases contained already in the acquired lidar signal from uncertainties and errors related to misleading assumptions needed in the optical properties retrieval algorithms.

In particular CALIPSO backscattered signals at 532 nm, the so called attenuated backscatter, can be checked by comparison with the CALIPSO-like attenuated backscatter at 532 nm calculated by means of PEARL. Since June 14, 2006, devoted measurements are performed at CNR-IMAA in coincidence with CALIPSO overpasses following the EARLINET strategy specifically designed for the CALIPSO measurements (Wandinger et al., 2008). During the first year of CALIPSO correlative measurements, we collected about 70 cases of PEARL measurements in coincidence with CALIPSO overpasses over Potenza within 100 km. A first analysis has been carried out for all of these data obtained in night-time conditions and in absence of low clouds. This choice allows us to consider only cases in which the aerosol extinction profile can be directly measured from PEARL and to avoid cases (low clouds) in which the variability is too high compared to the horizontal distance between CALIPSO overpass and PEARL. In retrieving attenuated backscatter profile from PEARL data, it has to be taken into account that PEARL and CALIPSO transmission terms are different, because the first lidar is an upward looking lidar and CALIPSO is a downward looking lidar. The molecular terms, backscatter coefficient and transmission, can be obtained by a co-located radiosounding if available or can be well approximated using atmospheric models. The ozone terms can be estimated starting from ozone profiles provided by Met Manager Weather Software and available directly by CALIPSO level 1 products, taking into account the ozone absorption in the Chappuis band at 532 nm (Brosseur et al., 2005). The mean profile (16 profiles of 30 minutes) of attenuated backscatter observed by CALIPSO and the analogous quantity measured by PEARL are reported in Figure 15. There is a good agreement between the two observations. The large difference in the PBL (about 50 %,)

indicated by the purple oval) can be partly ascribed to no-perfect spatial coincidence that makes the comparison in the PBL very difficult. A better agreement is achieved in the altitude range between 3 and 8 km, where the relative difference is always below 20 % that is the expected error in the CALIPSO vertical profiles. It is interesting to note that in the 3-8 km altitude range as well as in the lowest troposphere, CALIPSO typically underestimates PEARL measurements. This negative difference could be a signature of multiple scattering effects on CALIPSO signals. In summary we find the most relevant differences in cirrus clouds (green oval) and in the PBL.

Besides the average profile comparisons, a single profile comparison is also possible. In Figure 16 another case is reported of single profile comparison, averaged over 30 min, which shows a much better agreement between CALIPSO and PEARL in absence of cirrus clouds or of high aerosol load in the PBL. Some differences in the shape of the profiles are still present due to the non perfect collocation of the two measurements.

These are only some examples of the CALIPSO validation activity that show the relevance of this work for the CALIPSO mission. The involvements of all the EARLINET stations in such kind of studies will both improve the statistics and increase the probability of suppressing the differences that are due to the non perfect collocation of the instruments.

In the next years, similar validations studies will be performed involving a larger number of EARLINET stations and the corresponding data (after passing the quality assurance procedure) will be submitted to ESA's calibration/validation database (currently NADIR).

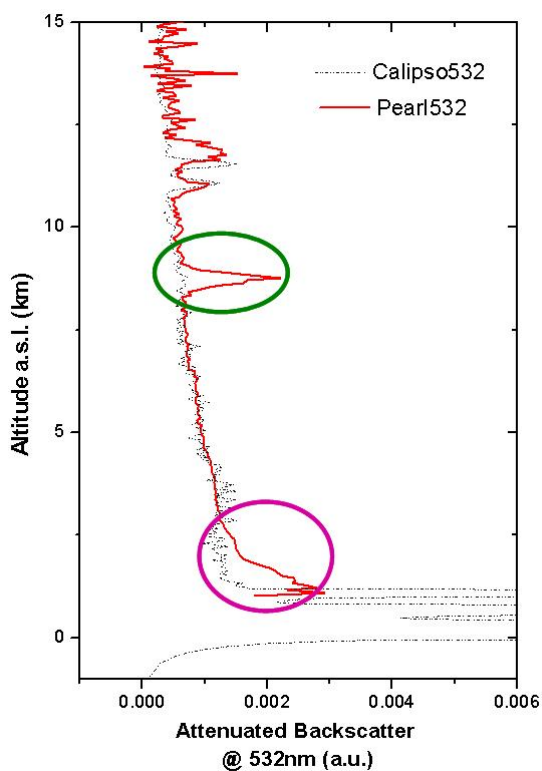


Figure 15: Mean profiles of attenuated backscatter at 532 nm as measured by CALIPSO and PEARL in night time low-clouds free conditions for relative distance lower than 100 km.

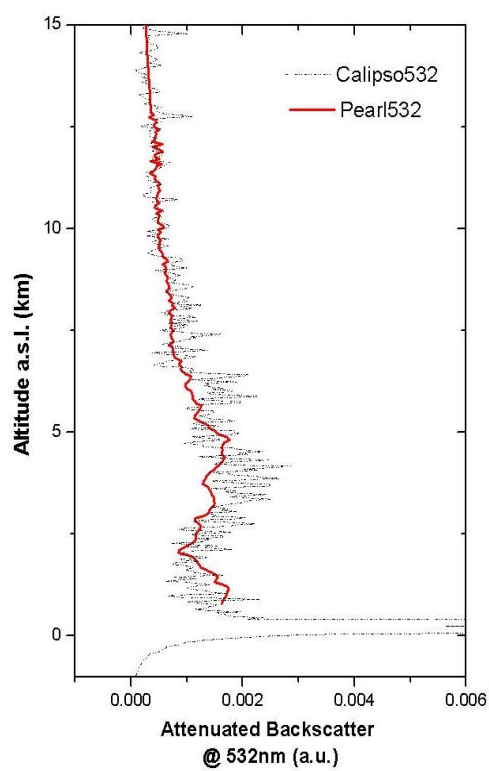


Figure 16: Example of single profile comparison of attenuated backscatter between CALIPSO and PEARL.

10 VALID-related presentations and publications

Several papers/presentations have been created reporting on the activities of the VALID project in 2008.

Various presentations have been given at quality working group meetings of GOMOS and SCIAMACHY.

- Two contributions have been prepared for the special issue on 25 years of the Montreal protocol in the International Journal of Remote Sensing (Steinbrecht et al., 2009, van Gijssel et al., 2009).
- One paper for the special issue on GOMOS in ACP is currently (2009) still in preparation.
- Results of the validation of CALIPSO have been submitted to ACP discussions (Mona et al., submitted).

Work was presented at the following conferences:

- Quadrennial ozone symposium (Bovensmann et al., 2008b, Steinbrecht et al., 2008a, van Gijssel et al., 2008)
- International laser radar conference (Mona et al., 2008, Pappalardo et al., 2008)
- 37th Committee on space research (Bovensmann et al., 2008a)
- AGU Fall meeting (Hauchecorne et al., 2008, Steinbrecht et al., 2008b)

11 Conclusions

One of the aims of this project has been to assess the quality of ENVISAT's ozone and temperature profiles with lidar data, and check for possible dependencies on certain parameters. One of the main objectives was to make lidar ozone and temperature profiles available for validation activities. Currently over 8300 profiles are stored in HDF-format in the correlative database at NILU. These profiles are quite evenly spread over the period July 2002 until the end of 2008, and cover several different global regions.

From data of the planned measurements for GOMOS, MIPAS and SCIAMACHY coincidences have been derived with the lidar stations and from the currently available lidar data we have derived listings of collocated measurements. Since the beginning of the VALID project, there is a significant improvement in the ENVISAT data availability, which resulted in several assessment studies and algorithm development support.

The current status of the validation activities is that an extensive analysis of ENVISAT data has been performed for GOMOS ozone, SCIAMACHY ozone profiles. The GOMOS H RTP and MIPAS (RR) ozone and temperature (scientific) profiles have been validated on a limited data set. A complete overview of the validation status of each instrument is provided in Table 11-1 and Table 11-2.

Table 11-1: Validation status of ENVISAT Data from IPF Processor		
Legend: = complete assessment, = initial assessment, = no assessment.		
<i>Instrument</i>	<i>Ozone version</i>	<i>Temperature version</i>
GOMOS	GOPR 6.0cf, IPF 5.0, GOPR 7.0ab	H RTP from GOPR 6.0cf
MIPAS FR	IPF 4.61/4.62	IPF 4.61/4.62
MIPAS OR	IPF 4.61/4.62	IPF 4.61/4.62
SCIAMACHY	IPF 3.01, prototype 4.x	not applicable

Table 11-2: Validation status of ENVISAT Data from 'Scientific' Processing		
Legend: = complete assessment, = initial assessment, = no assessment.		
<i>Instrument</i>	<i>Ozone version</i>	<i>Temperature version</i>
GOMOS	Only from prototype	Only from prototype
MIPAS FR + OR	University of Oxford MORSE 1.00, 1.01 and 1.02	University of Oxford MORSE 1.00, 1.01 and 1.02
SCIAMACHY	Stratozone 2.0	not applicable

Another part of VALID project is dedicated to aerosol and cloud studies. These studies are carried out by CNR-IMAA and involve lidar measurements from EARLINET. In the first year, three satellite instruments were identified as having aerosol products suitable for the comparison with lidar measurements, namely MODIS, OMI and CALIPSO. These satellites are considered to be the most widely used to study aerosol measurements. In the following years of the project, other satellites and instruments (such as MERIS, GOMOS and SCIAMACHY) will be considered and their aerosol and clouds products suitability for comparison with Raman lidar data will be evaluated.

12 References

- AMODEO, A., MATTIS, I., BÖCKMANN, C., D'AMICO, G., MÜLLER, D., OSTERLOH, L., CHAIKOVSKY, A., PAPPALARDO, G., ANSMANN, A., APITULEY, A., ALADOS-ARBOLEDAS, L., BALIS, D., COMERON, A., FREUDENTHALER, V., MITEV, V., NICOLAE, D., PAPAYANNIS, A., PERRONE, M. R., PIETRUCZUK, A., PUJADAS, M., PUTAUD, J. P., RAVETTA, F., RIZI, V., SIMEONOV, V., SPINELLI, N., STEBEL, K., STOYANOV, D., TRICKL, T. & WIEGNER, M. (2007) Optimization of lidar data processing: A goal of the EARLINET-ASOS project. *Proceedings of SPIE - The International Society for Optical Engineering*.
- ANSELMO, T., CLIFTON, R., HUNT, W. H., LEE, K.-P., MURRAY, T., POWELL, K. A., RODIER, S. D., VAUGHAN, M., CHOMETTE, O., VIOLLIER, M., HAGOLLE, O., LIFERMANN, A., GARNIER, A., PELON, J., CURREY, J. C., PITTS, M. & WINKER, D. (2007) Cloud - aerosol lidar infrared pathfinder satellite observations(CALIPSO), Data management system, data products catalog, release 2.4, document number: PC-SCI-503 (http://www-calipso.larc.nasa.gov/products/CALIPSO_DPC_Rev2x4.pdf)
- ANSMANN, A., RIEBESELL, M., WANDINGER, U., WEITKAMP, C., VOSS, E., LAHMANN, W. & MICHAELIS, W., 1992, Combined raman elastic-backscatter LIDAR for vertical profiling of moisture, aerosol extinction, backscatter, and LIDAR ratio. *Applied Physics B Photophysics and Laser Chemistry*, 55, **1**, 18-28.
- ANSMANN, A., RIEBESELL, M. & WEITKAMP, C., 1990, Measurement of atmospheric aerosol extinction profiles with a Raman lidar. *Optics Letters*, 15, **13**, 746-748.
- BARNES, W. L., PAGANO, T. S. & SALOMONSON, V. V., 1998, Prelaunch Characteristics of the Moderate Resolution Imaging Spectroradiometer (MODIS) on EOS-AM1. *IEEE Transactions on Geoscience and Remote Sensing*, 36, **4**, 1088-1100.
- BÖSENBERG, J., MATTHIAS, V., AMODEO, A., AMORIDIS, V., ANSMANN, A., BALDASANO, J. M., BALIN, I., BALIS, D., BÖCKMANN, C., BOSSELI, A., CARLSSON, G., CHAIKOVSKY, A., CHOURDAKIS, G., COMERON, A., TOMASI, F. D., EIXMANN, R., FREUDENTHALER, V., GIEHL, H., GRIGOROV, I., HAGARD, A., IARLORI, M., KIRSCH, A., KOLAROV, G., KOMGUEM, L., KREIPL, S., KUMPF, W., LARCHEVEQUE, G., LINNÉ, H., MATTHEY, R., MATTIS, I., MEKLER, A., MIRONOVA, I., MITEV, V., L. MONA, MÜLLER, D., MUSIC, S., NICKOVIC, S., PANDOLFI, M., PAPAYANNIS, A., PAPPALARDO, G., PELON, J., PEREZ, C., PERRONE, R. M., PERSSON, R., RESENDES, D. P., RIZI, V., ROCADENBUSCH, F., RODRIGUEZ, J. A., SAUVAGE, L., SCHNEIDENBACH, L., SCHUMACHER, R., V. SHCHERBAKOV, SIMEONOV, V., SOBOLEWSKI, P., SPINELLI, N., STACHLEWSKA, I., STOYANOV, D., TRICKL, T., TSAKNAKIS, G., VAUVHAN, G., WANDINGER, U., WANG, X., WIEGNER, M., ZAVRTANIK, M. & ZEREFOS, C. (2003) A European Aerosol Research Lidar Network to Establish an Aerosol Climatology: MPI-report 348. Hamburg (Germany), Max-Planck-Institut für Meteorologie.
- BOVENSMANN, H., ROZANOV, A., VON SAVIGNY, C., EICHMANN, K.-U., BRAMSTEDT, K., AMEKUDZI, L. K., BURROWS, J. P., DOICU, A., LICHTENBERG, G., GOTTWALD, M., VAN GIJSEL, J. A. E. & FEHR, T. (2008a) Monitoring of stratospheric O₃ and NO₂ profiles with SCIAMACHY/ENVISAT. *37th Committee on Space Research (COSPAR) Scientific Assembly*. Montréal, Canada.
- BOVENSMANN, H., ROZANOV, A., VON SAVIGNY, C., EICHMANN, K.-U., BRAMSTEDT, K., AMEKUDZI, L. K., BURROWS, J. P., DOICU, A., LICHTENBERG, G., GOTTWALD, M., VAN GIJSEL, J. A. E. & FEHR, T. (2008b) Monitoring of stratospheric O₃ and NO₂ profiles with SCIAMACHY/ENVISAT. *Quadrennial ozone symposium*. Tromsø, Norway.
- BRASSEUR, G. P. & SOLOMON, S. (2005) *Aeronomy of the Middle Atmosphere*, Dordrecht, the Netherlands, Reidel Publishing.
- FORSTER, P., RAMASWAMY, V., ARTAXO, P., BERNTSEN, T., BETTS, R., FAHEY, D. W., HAYWOOD, J., LEAN, J., LOWE, D. C., MYHRE, G., NGANGA, J., PRINN, R., RAGA, G., SCHULZ, M. & VAN DORLAND, R. (2007) Changes in Atmospheric Constituents and in Radiative Forcing. IN SOLOMON, S., QIN, D., MANNING, M., CHEN, Z.,

- MARQUIS, M., AVERYT, K. B., M.TIGNOR & MILLER, H. L. (Eds.) *Climate Change 2007: The physical science basis. Contribution of working group I to the Fourth assessment report of the Intergovernmental Panel on Climate Change*. Cambridge (United Kingdom) and New York (United States of America), Cambridge University Press.
- GORDON, H. R., 1990, Radiometric considerations for ocean color remote sensors. *Applied Optics*, 29, **22**, 3228-3236.
- GORDON, H. R. & MOREL, A. Y. (1983) *Remote assessment of ocean color for interpretation of satellite visible imagery: a review*, Springer-Verlag.
- GUIRLET, M. (2009) Comparison of GOMOS O3 profiles with other measurements - GOPR v6.0cf (7.0ab), slide 4. Presented at GOMOS quality working group meeting 19 in Paris (France) 9-10/02/2009.
- HAUCHECORNE, A., BERTAUX, J. L., DALAUDIER, F., KYRÖLÄ, E., TAMMINEN, J., SOFIEVA, V., FUSSEN, D., VANHELLEMONT, F., DE CLERCQ, C., LAMBERT, J.-C., FANTON D'ANDON, O., BARROT, G., GUIRLET, M., FEHR, T., SAAVEDRA DE MIGUEL, L. & VAN GIJSEL, A. (2008) Highlights of six-year GOMOS observations. *AGU Fall Meeting Atmospheric Sciences [A] 0340 Middle atmosphere: composition and chemistry, 2008*. San Francisco, USA.
- HOSTETLER, C. A., LIU, Z., REAGAN, J., VAUGHAN, M., WINKER, D., OSBORN, M., HUNT, W. H., POWELL, K. A. & TREPTE, C. (2006) Calibration and level 1 data products. *CALIOP algorithm theoretical basis document*. Hampton, Virginia (USA), NASA Langley Research Center.
- HUNT, L. A. (accessed 2009) CALIPSO data and tools available from the NASA Langley atmospheric science data center (<http://ams.confex.com/ams/pdfpapers/131600.pdf>).
- KING, M. D., HERRING, D. D. & DINER, D. J., 1995, Earth observing system: a space-based program for assessing mankind's impact on the global environment. *Optics and Photonics News*, 6, **1**, 34-39.
- KING, M. D., KAUFMAN, Y. J., MENZEL, W. P. & TANRÉ, D., 1992, Remote sensing of cloud, aerosol, and water vapor properties from the ModerateResolution Imaging Spectrometer (MODIS). *IEEE Transactions on Geoscience and Remote Sensing*, 30, **1**, 2-27.
- MATTHIAS, V., BALIS, D., BÖSENBERG, J., EIXMANN, R., IARLORI, M., KOMGUEM, L., MATTIS, I., PAPAYANNIS, A., PAPPALARDO, G., PERRONE, M. R. & WANG, X., 2004, Vertical aerosol distribution over Europe: Statistical analysis of Raman lidar data from 10 European Aerosol Research Lidar Network (EARLINET) stations. *Journal of Geophysical Research D: Atmospheres*, 109, **18**, D18201 1-12.
- MEIJER, Y. J., LOKKEMA, D. E. & SWART, D. P. J. (2005a) Overview of EQUAL Analysis Results (in support of ESL processor upgrade verification). *EQUAL project report series*. Bilthoven, RIVM.
- MEIJER, Y. J. & SWART, D. P. J. (2005b) Envisat Quality Assessment with Lidar: Annual report 2004. *EQUAL project report series*. Bilthoven, RIVM.
- MEIJER, Y. J., SWART, D. P. J., ALLAART, M., ANDERSEN, S. B., BODEKER, G., BOYD, I. S., BRAATHEN, G., CALISESI, Y., CLAUDE, H., DOROKHOV, V., GATHEN, P. V. D., GIL, M., GODIN-BEEKMANN, S., GOUTAIL, F., HANSEN, G., KARPETCHKO, A., KECKHUT, P., KELDER, H. M., KOELEMMEIJER, R., KOIS, B., KOOPMAN, R. M., KOPP, G., LAMBERT, J.-C., LEBLANC, T., MCDERMID, I. S., PAL, S., SCHETS, H., STUBI, R., SUORTTI, T., VISCONTI, G. & YELA, M., 2004, Pole-to-pole validation of Envisat GOMOS ozone profiles using data from ground-based and balloon sonde measurements. *Journal of Geophysical Research*, 109, D23305.
- MONA, L., AMODEO, A., BOSELLI, A., D'AMICO, G., GIUNTA, A., MADONNA, F., RUSSO, F. & PAPPALARDO, G., submitted, One year of CNR-IMAA multi-wavelength Raman lidar measurements in correspondence of CALIPSO overpass: level 1 products comparison. *Atmospheric Chemistry and Physics - discussions*.
- MONA, L., AMODEO, A., BOSELLI, A., D'AMICO, G., MADONNA, F. & PAPPALARDO, G. (2008) Systematic multi-wavelength Raman measurements: a reference for aerosol study. *24th international laser radar conference*. Boulder, Colorado (USA).

- MONA, L., AMODEO, A., PANDOLFI, M. & PAPPALARDO, G., 2006, Saharan dust intrusions in the Mediterranean area: Three years of Raman lidar measurements. *Journal of Geophysical Research D: Atmospheres*, 111, **16**, D16203, doi: 10.1029/2005JD006569.
- MÜLLER, D., ANSMANN, A., MATTIS, I., TESCHE, M., WANDINGER, U., ALTHAUSEN, D. & PISANI, G., 2007, Aerosol-type-dependent lidar ratios observed with Raman lidar. *Journal of Geophysical Research D: Atmospheres*, 112, **16**, D16202, doi:10.1029/2006JD008292.
- MÜLLER, D., HEINOLD, B., TESCHE, M., TEGEN, I., ALTHAUSEN, D., ARBOLEDAS, L. A., AMIRIDIS, V., AMODEO, A., ANSMANN, A., BALIS, D., COMERON, A., D'AMICO, G., GERASOPOULOS, E., GUERRERO-RASCADO, J. L., FREUDENTHALER, V., GIANNAKAKI, E., HEESE, B., IARLORI, M., KNIPPERTZ, P., MAMOURI, R. E., MONA, L., PAPAYANNIS, A., PAPPALARDO, G., PERRONE, R. M., PISANI, G., RIZI, V., SICARD, M., SPINELLI, N., TAFURO, A. & WIEGNER, M., 2009, EARLINET observations of the 14-22-May long-range dust transport event during SAMUM 2006: Validation of results from dust transport modelling. *Tellus, Series B: Chemical and Physical Meteorology*, 61, **1**, 325-339.
- NATIONAL AERONAUTICS AND SPACE ADMINISTRATION (NASA) (2007) OMAERUV readme file (http://daac.gsfc.nasa.gov/documents/OMAERUV_README_File_v3.doc).
- NATIONAL AERONAUTICS AND SPACE ADMINISTRATION (NASA) (2009) CALIPSO - Cloud-aerosol lidar and infrared pathfinder satellite observations (<http://www-calipso.larc.nasa.gov>).
- PAPAYANNIS, A., AMIRIDIS, V., MONA, L., TSAKNAKIS, G., BALIS, D., BÖSENBERG, J., CHAIKOVSKI, A., DE TOMASI, F., GRIGOROV, I., MATTIS, I., MITEV, V., MÜLLER, D., NICKOVIC, S., PÉREZ, C., PIETRUCZUK, A., PISANI, G., RAVETTA, F., RIZI, V., SICARD, M., TRICKL, T., WIEGNER, M., GERDING, M., MAMOURI, R. E., D'AMICO, G. & PAPPALARDO, G., 2008, Systematic lidar observations of Saharan dust over Europe in the frame of EARLINET (2000-2002). *Journal of Geophysical Research D: Atmospheres*, 113, **10**, D10204, doi: 10.1029/2007JD009028.
- PAPPALARDO, G., BÖSENBERG, J., AMODEO, A., ANSMANN, A., APITULEY, A., ARBOLEDAS, L. A., BALIS, D., BOCKMAN, C., COMERON, A., D'AMICO, G., FREUDENTHALER, V., GRIGOROV, I., HANSEN, G., LINNÈ, H., MATTIS, I., MONA, L., MÜLLER, D., MITEV, V., NICOLAE, D., PAPAYANNIS, A., PERRONE, M. R., PIETRUCZUK, A., PUJADAS, M., PUTAUD, J.-P., RAVETTA, F., RIZI, V., SIMEONOV, V., SPINELLI, N., TRICKL, T., WANDINGER, U. & WIEGNER, M. (2008) EARLINET for long term observations of aerosol over Europe. *24th international laser radar conference*. Boulder, Colorado (USA).
- ROYAL NETHERLANDS METEOROLOGICAL INSTITUTE (KNMI) (2008) Ozone Monitoring Instrument (<http://www.knmi.nl/omi/research/instrument/index.php>).
- RUNNING, S. W., JUSTICE, C. O., SALOMONSON, V. V., HALL, D., BARKER, J., KAUFMAN, Y. J., STRAHLER, A., HUETE, A. R., MULLER, J.-P., VANDERBILT, V., WAN, Z., TEILLET, P. & CARNEGIE, D., 1994, Terrestrial remote sensing, science and algorithms planned for EOS/MODIS. *International Journal of Remote Sensing*, 15, **17**, 3587-3620.
- SALOMONSON, V. V. & TOLL, D. L., 1991, Execution phase (C/D) spectral band characteristics of the EOS Moderate Resolution Imaging Spectrometer-NADIR (MODIS-N) facility instrument. *Advances in Space Research*, 11, **3**, 231-236.
- STEINBRECHT, W., CLAUDE, H., SCHÖNENBORN, F., MCDERMID, I. S., LEBLANC, T., GODIN, S., KECKHUT, P., VAN GIJSEL, J. A. E., SWART, D. P. J., BODEKER, G. E., PARRISH, A., BOYD, I. S., KÄMPFER, N., HOCKE, C., STOLARSKI, R. S., FRITH, S. M., THOMASON, L. W., REMSBERG, E. E., VON SAVIGNY, C. & BURROWS, J. P., 2009, Ozone and temperature trends in the upper stratosphere at five stations of the Network for the Detection of Atmospheric Composition Change. *International Journal of Remote Sensing*, in press.
- STEINBRECHT, W., CLAUDE, H., SCHÖNENBORN, F., MCDERMID, S., LEBLANC, T., GODIN-BEEKMANN, S., KECKHUT, P., HAUCHECORNE, A., VAN GIJSEL, J. A., SWART, D. P., BODEKER, G. E., PARRISH, A., BOYD, I. S., KÄMPFER, N., HOCKE, K., STOLARSKI, R. S., FRITH, S., THOMASON, L. W., REMSBERG, E. E., VON SAVIGNY, C., BURROWS, J. P., EYRING, V. & SHEPHERD, T. G. (2008a) Ozone and temperature trends in the upper

- stratosphere at five stations of the Network for the detection of atmospheric composition change. *Quadrennial ozone symposium*. Tromso, Norway.
- STEINBRECHT, W., CLAUDE, H., SCHÖNENBORN, F., MCDERMID, S., LEBLANC, T., GODIN-BEEKMANN, S., KECKHUT, P., HAUCHECORNE, A., VAN GIJSEL, J. A., SWART, D. P., BODEKER, G. E., PARRISH, A., BOYD, I. S., KÄMPFER, N., HOCKE, K., STOLARSKI, R. S., FRITH, S., THOMASON, L. W., REMSBERG, E. E., VON SAVIGNY, C., BURROWS, J. P., EYRING, V. & SHEPHERD, T. G. (2008b) Ozone and temperature trends in the upper stratosphere at five stations of the Network for the detection of atmospheric composition change. *AGU Fall Meeting Atmospheric Sciences [A] 0340 Middle atmosphere: composition and chemistry / 0394 Instruments and techniques / 1610 Atmosphere (0315, 0325) / 1616 Climate variability (1635, 3305, 3309, 4215, 4513)*. San Francisco (USA).
- SUSSKIND, J., ROSENFELD, J., REUTER, D. & CHAHINE, M. T., 1984, Remote Sensing of Weather and Climate Parameters from HIRS2/MSU on TIROS-N. *Journal of Geophysical Research*, 89, **D3**, 4677-4697.
- VAN GIJSEL, J. A. E., SWART, D. P. J., BARAY, J.-L., CLAUDE, H., FEHR, T., VON DER GATHEN, P., GODIN-BEEKMANN, S., HANSEN, G., LEBLANC, T., MCDERMID, I. S., MEIJER, Y. J., NAKANE, H., QUEL, E., STEINBRECHT, W., STRAWBRIDGE, K., TATAROV, B. & WOLFRAM, E., 2009, Global validation of ENVISAT ozone profiles using lidar measurements. *International Journal of Remote Sensing*, in press.
- VAN GIJSEL, J. A. E., SWART, D. P. J., BARAY, J.-L., CLAUDE, H., FEHR, T., VON DER GATHEN, P., GODIN-BEEKMANN, S., HANSEN, G., LEBLANC, T., MCDERMID, I. S., NAKANE, H., QUEL, E., STEINBRECHT, W., STRAWBRIDGE, K. & WOLFRAM, E. (2008) Pole-to-pole validation of ENVISAT ozone profiles using data from lidar measurements. *Quadrennial ozone symposium*. Tromso, Norway.
- VEIHELMANN, B. & VEEFKIND, J. P. (2007) OMAERO readme file (www.knmi.nl/omi/research/product/aerosol/omaero_Readme.pdf).
- WANDINGER, U., ANSMANN, A., MATTIS, I., MÜLLER, D. & PAPPARLARO, G. (2008) CALIPSO and beyond: long-term ground-based support of space-borne aerosol and cloud lidar missions. *24th international laser radar conference*. Boulder, Colorado (USA).

13 Appendix 1: The EARLINET database

The EARLINET database represents, up to now, the largest collection of data for the aerosol distribution on European scale. The data quality of the database is assured by the EARLINET data quality program which includes activities such as the intercomparison of algorithms and lidar systems.

13.1 Database content

The general content of the database consists of (see below for the definitions):

- vertical profiles of aerosol backscattering coefficient at 355, 532 and 1064 nm (some stations also at 351 and 694 nm)
- vertical profiles of aerosol extinction coefficient at 355, and 532 nm
- vertical profiles of Lidar Ratio at 355, 532 nm
- vertical profiles of Depolarization Ratio at 532 nm
- dust layer height
- mixing layer height
- time series of vertical profiles are reported for diurnal cycle observations

The EARLINET database contains two kinds of files: e-files and b-files.

e-files

These files contain vertical profiles of aerosol backscattering coefficient and of aerosol extinction coefficient retrieved independently without a-priori hypothesis on existing relation between them. The aerosol extinction coefficient is retrieved directly from Raman lidar measurements or from lidar multi angle measurements. The aerosol backscattering coefficient is retrieved from the combination of Raman and elastic lidar measurements. Both parameters are reported with the same vertical resolution and with their statistical errors.

b-files

These files contain vertical profiles of aerosol backscattering coefficient. This coefficient has been retrieved:

- from only elastic lidar signal, with hypothesis on vertical profile of Lidar Ratio on the base of literature or of local climatological studies. In this case, the vertical profile of the Lidar Ratio (or the constant value used) is also included.
- from the combination of Raman and elastic measurements, but with a resolution higher than the corresponding reported in e-files. In fact, the improvement of the quality of aerosol extinction coefficient to be reported in e-files requires a degradation of the resolution.

Further parameters can be included:

- vertical profiles of aerosol depolarization ratio
- vertical profiles of aerosol extinction coefficient (obtained by multiplying the aerosol backscattering profile for the corresponding assumed Lidar Ratio profile)
- dust layer height
- mixing layer height

All the files include other information such as: geographic coordinates of the lidar station, time duration of the measurement, effective spatial resolution, used wavelengths, analysis technique used and possible related assumptions, possible ancillary information used, comments related to the measurement.

The files are stored as single profile file (containing aerosol optical profile(s) at a fixed time) and as a time series file (containing aerosol optical profile(s) at different times).

13.1.1 Single profile file NetCDF structure

Variables:

Name	Type	Scalar/Vector	Dim=length	Mandatory/Optional	Units	Alternative name
Altitude	Double	V	*	M	m	Height above sea level
Backscatter	Double	V	*	M	$\frac{1}{m \cdot sr}$	
Extinction	Double	V	*	M	$\frac{1}{m}$	
ErrorBackscatter	Double	V	*	O	$\frac{1}{m \cdot sr}$	
ErrorExtinction	Double	V	*	O	$\frac{1}{m}$	
DustLayerHeight	Double	S		O	m	
MixingLayerHeight	Double	S		O	m	
WaterVaporMixingRatio	Double	V	*	O	$\frac{g}{kg}$	
ErrorWaterVapor	Double	V	*	O	-	
Depolarisation	Double	V	*	O	-	
RayleighExtinction	Double	V	*	O	-	

Global attributes (all mandatory):

Name: System	Type=text
Name: Location	Type=text
Name: Longitude_degrees_east	Type=double
Name: Latitude_degrees_north	Type=double
Name: Altitude_meter_asl	Type=double
Name: EmissionWavelength_nm	Type=double
Name: DetectionWavelength_nm	Type=double
Name: DetectionMode	Type=text
Name: ZenithAngle_degrees	Type=double
Name: ShotsAveraged	Type=integer
Name: ResolutionRaw_meter	Type=double
Name: ResolutionEvaluated	Type=text
Name: StartDate	Type=integer
Name: StartTime_UT	Type=integer
Name: StopTime_UT	Type=integer
Name: EvaluationMethod	Type=text
Name: InputParameters	Type=text
Name: Comments	Type=text

13.1.2 Timeseries NetCDF file structure

Variables:

Name	Type	Dim=length	Dim=time	Mandatory/ Optional	Units	Alternative name
Altitude	Double	*		M	m	Height above sea level
Time	Double		*	M	s	Seconds since start of measurement
Backscatter	Double	*	*	M	$\frac{1}{m \cdot sr}$	
Extinction	Double	*	*	M	$\frac{1}{m}$	
ErrorBackscatter	Double	*	*	O	$\frac{1}{m \cdot sr}$	
ErrorExtinction	Double	*	*	O	$\frac{1}{m}$	
DustLayerHeight	Double		*	O	m	
MixingLayerHeight	Double		*	O	m	
WaterVaporMixingRatio	Double	*	*	O	$\frac{g}{kg}$	
ErrorWaterVapor	Double	*	*	O	-	
Depolarisation	Double	*	*	O	-	
RayleighExtinction	Double	*	*	O	-	

Global attributes (all mandatory):

Name: System	Type=text
Name: Location	Type=text
Name: Longitude_degrees_east	Type=double
Name: Latitude_degrees_north	Type=double
Name: Altitude_meter_asl	Type=double
Name: EmissionWavelength_nm	Type=double
Name: DetectionWavelength_nm	Type=double
Name: DetectionMode	Type=text
Name: ZenithAngle_degrees	Type=double
Name: ShotsAveraged	Type=integer
Name: ResolutionRaw_meter	Type=double
Name: ResolutionEvaluated	Type=text
Name: StartDate	Type=integer
Name: StartTime_UT	Type=integer
Name: StopTime_UT	Type=integer
Name: EvaluationMethod	Type=text
Name: InputParameters	Type=text
Name: Comments	Type=text

13.2 File naming conventions

Filenames for the evaluated aerosol profiles (extinction and backscattering) follow this convention:

ooyyMMddhhmm.tw

with:

oo: originator code (see below)
yy: year since 2000
MM: month of the year (1-12) (referred to the start-time of the measurement)
dd: day of month (1-31) (referred to the start-time of the measurement)
hh: hour of day (0-23) (referred to the start-time of the measurement)
mm: minute of hour (0-59) (referred to the start-time of the measurement)
t: type code (e = extinction, b = backscatter)
w: wavelength given in nm (for Raman measurements the emitted wavelength is reported).

The **originator code** is as follows:

<i>ab</i> : Aberystwyth	<i>gp</i> : Garmisch-Partenkirchen	<i>la</i> : L'Aquila	<i>mu</i> : Munich
<i>an</i> : Andoya	<i>gr</i> : Granada	<i>lc</i> : Lecce	<i>na</i> : Napels
<i>at</i> : Athens	<i>hb</i> : Hamburg Bergedorf	<i>le</i> : Leipzig	<i>ne</i> : Neuchatel
<i>ba</i> : Barcelona	<i>hb</i> : Hamburg	<i>li</i> : Lisboa	<i>ox</i> : Oxyolithos
<i>be</i> : Belsk	<i>hp</i> : Haute-Provence	<i>lk</i> : Linköping	<i>pl</i> : Palaiseau
<i>bb</i> : Bilthoven	<i>is</i> : Ispra	<i>ma</i> : Madrid	<i>po</i> : Potenza
<i>bu</i> : Bucharest	<i>ju</i> : Jungfraujoch	<i>mi</i> : Minsk	<i>sf</i> : Sofia
<i>ca</i> : Cabauw	<i>kb</i> : Kühlungsborn	<i>ms</i> : Maisach	<i>th</i> : Thessaloniki

13.3 Database organization

EARLINET systematic measurements are collected on the base of a fixed measurement scheduling. This consists of three measurements per week performed simultaneously by all the network stations: one measurement is performed at 12:00 UT, and two measurements at sunset. The two selected measurement times are representative of two different situations: the first one, when the convective activity is at its maximum and the second one when the convective activity is stopping. These are measurements performed systematically at all the stations and are used to carry out climatological studies.

Additional measurements are performed to address specifically important processes that are localised either in space or time, such as Saharan dust outbreaks, forest fires, volcanic eruptions, photochemical smog.

Further measurements are the correlative measurements for CALIPSO performed following an ad hoc strategy established within EARLINET.

The files are divided in different categories related to regular and special observations:

- *climatology*: routine measurements (according the scheduled three times a week) to establish the climatology
- *saharan_dust*: special observations of Saharan dust outbreaks following the alert system based on dust forecast
- *forest_fires*: observations in correspondence of large forest fires
- *photosmog*: observations of photochemical smog episodes in large cities
- *rural_urban*: nearly simultaneous measurements at pairs of stations that are sufficiently close to minimize the effect of large scale patterns, but sufficiently apart to reflect the differences in the surrounding: urban versus rural or pre-rural
- *diurnal_cycles*: observations of diurnal cycle of aerosols in the boundary layer

- *stratosphere*: stratospheric aerosol observations and detection of smaller scale features of stratospheric aerosol distribution and its interdependence with dynamics and heterogeneous chemistry
- *etna*: observations of the Etna eruption events in 2001 and 2002
- *cirrus*: observations of cirrus clouds
- *calipso*: correlative measurements in coincidence of the CALIPSO overpasses.

13.4 Definition of the parameters

When laser radiation with power P_L at wavelength λ_L is sent into atmosphere, part of the radiation is backscattered. The optical power $P(\lambda, \lambda_L, R)$ of the backscattered radiation received from the distance R at wavelength λ depends on atmospheric composition through two parameters: the backscattering coefficient and the extinction coefficient, and is described by the lidar equation:

$$P(\lambda, \lambda_L, R) \sim \frac{P_L}{R^2} \beta(\lambda, \lambda_L, R) \exp\left(-\int_0^R \alpha(\lambda, R') dR'\right) \exp\left(-\int_0^R \alpha(\lambda_L, R') dR'\right)$$

Backscattering coefficient β

Extinction coefficient α

The **backscattering coefficient** is the fraction of incident radiation backscattered for unitary solid angle and for unitary length [$\text{m}^{-1} \text{sr}^{-1}$].

It depends on the kind of scattering process: elastic (at λ_i) or inelastic (at $\lambda \neq \lambda_i$).

It is due to contributions of both gas (g) and particles (p) of atmosphere:

$$\beta = \beta_g + \beta_p.$$

In the database only the particle contribution β_p is reported.

The **extinction coefficient** is defined as the energy flux reduction per unitary path [m^{-1}].

It gives a measurement of the energy loss of the laser beam in the atmosphere.

It is due to contributions of both gas (g) and particles (p) of atmosphere deriving from both the scattering (s) and absorption (a) processes:

$$\alpha = (\alpha_{g,s} + \alpha_{p,s}) + (\alpha_{g,a} + \alpha_{p,a}).$$

In the database the only the particle contribution is reported.

The extinction coefficient integrated over a spatial path provides the *optical depth*:

$$\tau(\lambda_L, R) = \int_0^R \alpha(\lambda_L, R') dR'$$

The **lidar ratio** is defined as the ration between the aerosol extinction coefficient and the aerosol backscatter coefficient:

$$LR(\lambda_L, R) = \frac{\alpha(\lambda_L, R)}{\beta(\lambda_L, R)}$$

This is a parameter strongly related to the microphysical properties of the aerosols: aerosol type, size distribution, relative humidity. Unlike α and β , LR doesn't depend on aerosol amount, but only on aerosol kind.

Lidar measurements of atmospheric depolarization can be used to distinguish between liquid and solid phases of water in the atmosphere. It can also be used to distinguish between aerosols that are highly irregularly shaped, such as for example desert dust, and aerosol that have a more spherical shape. The quantity to describe the degree of polarization is the linear **depolarization**

ratio $\delta = I_{\perp} / I_{\parallel}$, where I_{\perp} and I_{\parallel} are the measured perpendicular and parallel backscatter intensities with respect to the transmitter polarization axis.

The **mixing layer height** is defined as the lowest layer where turbulent mixing processes establish an exchange between the surface layer and the atmosphere above. When aerosol is used as a tracer, e.g. in lidar measurements, the top of this layer can be identified by the lowest clearly defined minimum of $d/dR (PR^2)$, where PR^2 is the range corrected lidar signal P .

The **dust layer height** is defined as the lowest layer that generally contains most of the aerosols except special elevated layers like Saharan dust etc. Within EARLINET, the dust layer is considered as the mixing layer plus the residual layer, if that exists. The top of this layer can again be identified by a minimum of $d/dR (PR^2)$ (where PR^2 is the range corrected lidar signal P), but the existence of mixing processes is not required. If several layers exist that are clearly separated, only the lowest layer is labelled "dust layer". In the morning, when both the mixing layer and the residual layer on top of it may exist, these layers are typically well connected, but 2 local minima of $d/dR (PR^2)$ are observed.

14 Appendix 2: Overview of submission statistics - tables

In this section we give an overview of the lidar data submitted to the ENVISAT Cal/Val database at NILU in table format. In Table 14-1 we present the number of days (661) with measurements during the Commissioning Phase of ENVISAT, and most of these data have been submitted prior to the VALID project. In Table 14-2 we present the statistics for the data measured in 2003. Although the VALID project formally started in January 2004, the project partners additionally contributed data of 2003 and hence filled the gap between the end of the Commissioning Phase and the start of the project, which is a bonus for the project and amounts in total an extra 1259 days with measurements. In Table 14-3 we present the data measured in 2004, which come to a total of 1385 days. In Table 14-4 we present the data measured in 2005, which come to a total of 1287 days with measurements. In Table 14-5 we present the data measured in 2006, which now come to a total of 1331 days with measurements submitted to the database and Table 14-6 presents the data from 2007 with a total of 1226 measurements. In Table 14-7, the data for 2008 is presented with a total of 1042 measurements so far. Note that not all data has been submitted yet and that some differences for previous years can be found when comparing with the annual reports (2004-2006) and EQUAL final report (2007) due to new submissions and re-processing.

Station	System	Jul.	Aug.	Sept.	Oct.	Nov.	Dec.	Total
ALO	NILU001	0	0	7	11	13	8	39
ALO	NILU002	0	0	4	6	10	9	29
ESR	UBONN003	10	19	0	0	0	0	29
HOH	DWD001	5	7	8	4	6	3	33
HOH	DWD002	5	8	8	4	6	3	34
LAR	LPA001	0	0	2	0	0	0	2
LAR	LPA002	7	5	8	7	0	0	27
LAU	RIVM002	10	13	9	8	6	2	48
LAU	RIVM003	0	0	0	0	0	0	0
MLO	CNRS.SA004	9	15	15	3	10	9	61
MLO	CNRS.SA005	14	15	15	3	10	9	66
NYA	AWI001	0	0	0	11	6	11	28
NYA	AWI002	0	0	0	5	3	12	20
OHP	l_CNRS.SA001	13	15	14	10	11	6	69
OHP	r_CNRS.SA001	7	0	3	9	12	9	40
TMF	CNRS.SA003	13	16	2	9	11	10	61
TMF	CNRS.SA002	13	17	2	9	13	16	70
TOR	MSC001	2	0	1	2	0	0	5
TOTAL all systems		108	130	98	101	117	107	661

Note that submission of data for Lauder (temperature) is still foreseen after completion of the temperature retrieval scripts. The system in Toronto broke down in 2002 and has not been submitting measurements beyond 2002.

Station	System	Jan.	Feb.	Mar.	Apr.	May	Jun.	Jul.	Aug.	Sept.	Oct.	Nov.	Dec.	Total
ALO	NILU001	4	5	11	12	0	0	0	0	3	6	1	4	50
ALO	NILU002	4	3	7	12	0	0	0	1	3	5	1	4	32
ESR	UBONN003	9	1	0	0	0	0	4	0	1	1	0	0	32
HOH	DWD001	3	7	10	10	8	6	9	9	8	9	4	10	108
HOH	DWD002	4	7	10	10	8	6	9	9	8	9	4	10	111
LAR	LPA001	0	0	0	0	0	2	5	0	3	0	1	1	0
LAR	LPA002	2	8	11	11	7	15	6	5	14	12	9	5	90
LAU	RIVM002	7	8	7	9	5	5	11	8	9	11	3	2	59
LAU	RIVM003	0	0	0	0	0	0	0	0	0	0	0	0	0
MLO	CNRS.SA004	16	10	13	5	End	-	-	-	-	-	-	-	44
MLO	NASA.JPL001	-	-	-	Start	12	15	13	11	13	0	11	8	83
MLO	CNRS.SA005	16	10	14	5	End	-	-	-	-	-	-	-	45
MLO	NASA.JPL002	-	-	Start	1	14	15	13	11	16	8	11	8	97
NYA	AWI001	0	0	0	0	0	0	0	0	0	0	8	6	35
NYA	AWI002	13	9	0	0	0	0	0	0	0	0	3	2	41
OHP	l_CNRS.SA001	11	11	15	10	12	5	11	14	17	2	11	7	84
OHP	r_CNRS.SA001	3	9	17	13	12	15	15	0	11	8	14	7	111
TMF	CNRS.SA003	10	5	13	7	End	-	-	-	-	-	-	-	35
TMF	NASA.JPL003	-	-	-	Start	9	12	1	5	9	13	7	7	63
TMF	CNRS.SA002	14	5	13	8	End	-	-	-	-	-	-	-	40
TMF	NASA.JPL004	-	-	Start	1	10	13	3	5	9	14	9	8	72
TSU	NIES001	3	5	3	2	0	0	0	0	0	0	0	2	15
TSU	NIES002	3	4	1	2	0	0	0	0	0	0	0	2	12
TOTAL	all systems	172	138	115	65	79	90	75	92	110	97	114	112	1259

Note that submission of data for Lauder (temperature) is still foreseen.

Table 14-3: Data submission statistics, 2004 (in grey temperature lidar systems)

Station	System	Jan.	Feb.	Mar.	Apr.	May	Jun.	Jul.	Aug.	Sept.	Oct.	Nov.	Dec.	Total
ALO	NILU001	4	5	11	12	0	0	0	0	3	6	1	4	46
ALO	NILU002	4	3	7	12	0	0	0	1	3	5	1	4	40
ESR	UBONN003	9	1	0	0	0	0	4	0	1	1	0	0	16
EUR	MSC003	0	9	5	0	0	0	0	0	0	0	0	0	14
EUR	MSC004	0	9	5	0	0	0	0	0	0	0	0	0	14
HOH	DWD001	3	7	10	10	8	6	9	9	8	9	4	10	93
HOH	DWD002	4	7	10	10	8	6	9	9	8	9	4	10	94
LAR	LPA001	0	0	0	0	0	2	5	0	3	0	1	1	12
LAR	LPA002	2	8	11	11	7	15	6	5	14	12	9	5	105
LAU	RIVM002	7	8	7	9	5	5	11	8	9	11	5	3	88
LAU	RIVM003	0	0	0	0	0	0	0	0	0	0	0	0	0
MLO	NASA.JPL001	10	11	7	12	11	14	14	15	15	9	10	9	137
MLO	NASA.JPL002	10	11	7	12	11	14	14	15	15	9	10	9	137
NYA	AWI001	0	0	0	0	0	0	0	0	0	0	8	6	14
NYA	AWI002	13	9	0	0	0	0	0	0	0	0	3	2	27
OHP	l_CNRS.SA001	11	11	15	10	12	5	11	14	17	2	11	7	126
OHP	r_CNRS.SA001	3	9	17	13	12	15	15	0	11	8	14	7	124
TMF	NASA.JPL003	8	8	14	7	8	10	11	2	10	5	7	6	96
TMF	NASA.JPL004	12	8	14	13	13	17	12	4	11	9	10	10	133
TSU	NIES001	4	3	2	4	4	2	3	3	4	6	3	4	42
TSU	NIES002	2	0	1	3	1	2	2	3	3	5	1	4	27
TOTAL	all systems	106	127	143	138	100	113	126	88	135	106	102	97	1385

Note that submission of data for Lauder (temperature) is still foreseen.

Table 14-4: Data submission statistics, 2005 (in grey temperature lidar systems)

Station	System	Jan.	Feb.	Mar.	Apr.	May	Jun.	Jul.	Aug.	Sept.	Oct.	Nov.	Dec.	Total
ALO	NILU001	6	6	1	4	1	0	2	1	1	3	8	9	42
ALO	NILU002	6	6	1	2	0	0	0	0	1	3	7	8	34
DDU	CNRS.SA007	0	0	0	0	0	0	0	0	0	0	0	0	0
DDU	RMR_CNRS.SA002	0	0	0	0	0	0	0	0	0	0	0	0	0
ESR	UBONN003	7	0	0	0	0	0	14	1	0	0	0	0	22
EUR	MSC003	0	5	4	0	0	0	0	0	0	0	0	0	9
EUR	MSC004	0	5	4	0	0	0	0	0	0	0	0	0	9
HOH	DWD001	8	3	8	8	6	6	9	7	9	16	5	6	91
HOH	DWD002	8	3	8	8	6	6	9	7	9	17	5	6	92
LAR	LPA001	0	2	2	1	0	0	0	0	0	0	2	3	10
LAR	LPA002	5	11	5	6	16	17	6	10	16	11	4	1	108
LAU	RIVM002	5	5	5	5	2	4	6	5	5	5	6	3	56
LAU	RIVM003	0	0	0	0	0	0	0	0	0	0	0	0	0
MLO	NASA.JPL001	13	9	12	11	13	10	5	16	14	16	8	10	137
MLO	NASA.JPL002	13	9	13	11	13	10	5	16	14	16	8	10	138
NYA	AWI001	0	0	3	0	0	0	0	0	0	0	0	0	3
NYA	AWI002	4	2	3	0	0	0	0	0	0	0	0	0	9
OHP	l_CNRS.SA001	17	17	4	4	8	10	11	9	10	3	9	11	113
OHP	r_CNRS.SA001	18	18	16	17	9	9	15	15	20	6	14	16	173
RGH	CEILAP001	0	0	0	0	0	0	0	9	10	6	4	0	29
TMF	NASA.JPL003	5	4	9	1	5	12	7	3	8	14	12	4	84
TMF	NASA.JPL004	6	8	12	2	10	14	8	3	10	14	12	7	106
TSU	NIES001	4	0	2	0	1	0	1	2	2	1	0	0	13
TSU	NIES002	4	0	1	0	0	0	1	1	1	1	0	0	9
TOTAL all systems		126	113	113	80	90	98	99	105	130	132	104	94	1287

Note that submissions of data for Lauder (temperature) are still foreseen.

Table 14-5: Data submission statistics, 2006 (in grey temperature lidar systems)

Station	System	Jan.	Feb.	Mar.	Apr.	May	Jun.	Jul.	Aug.	Sept.	Oct.	Nov.	Dec.	Total
ALO	NILU001	3	4	10	2	0	0	0	2	5	8	2	2	38
ALO	NILU002	3	4	9	1	0	0	0	2	5	8	1	1	34
DDU	CNRS.SA007	0	0	0	0	0	0	0	0	0	0	0	0	0
DDU	RMR_CNRS.SA002	0	0	0	0	0	0	0	0	0	0	0	0	0
ESR	UBONN003	9	0	0	0	0	0	0	12	0	0	0	0	21
EUR	CARE.EC.STB001	0	5	0	0	0	0	0	0	0	0	0	0	5
EUR	CARE.EC.STB002	0	5	0	0	0	0	0	0	0	0	0	0	5
HOH	DWD001	10	4	5	5	9	8	12	4	8	11	5	10	91
HOH	DWD002	10	4	7	5	9	8	12	4	8	11	5	10	93
LAR	LPA001	1	1	5	4	5	2	0	0	0	0	0	1	19
LAR	LPA002	0	7	1	0	5	16	9	13	15	18	12	3	99
LAU	RIVM002	6	5	5	5	6	6	6	6	4	6	5	4	64
LAU	RIVM003	0	0	0	0	0	0	0	0	0	0	0	0	0
MLO	NASA.JPL001	13	0	3	10	14	14	16	18	15	12	12	11	138
MLO	NASA.JPL002	14	0	3	10	14	14	16	18	15	12	12	11	139
NYA	AWI001	0	0	0	0	0	0	0	0	0	0	0	0	0
NYA	AWI002	0	0	0	0	0	0	0	0	0	0	0	0	0
OHP	l_CNRS.SA001	12	7	9	12	11	14	9	14	15	10	14	11	138
OHP	r_CNRS.SA001	15	13	13	15	13	17	12	18	17	15	14	13	175
RGA	CEILAP001	1	1	3	5	5	3	1	8	6	12	3	3	51
TMF	NASA.JPL003	8	8	3	6	10	6	9	13	11	8	7	0	89
TMF	NASA.JPL004	9	9	6	8	12	6	9	13	11	9	11	0	103
TSU	NIES001	1	1	1	2	0	0	0	0	0	4	5	4	18
TSU	NIES002	1	0	1	0	0	0	0	0	0	2	4	2	4
TOTAL all systems		116	78	84	90	113	114	111	145	135	146	108	86	1331

Note that submissions of data for Dumont d'Urville (temperature), Ny Ålesund (temperature and ozone) and Lauder (temperature) are still foreseen.

Table 14-6: Data submission statistics, 2007 (in gray temperature lidar systems)

Station	System	Jan.	Feb.	Mar.	Apr.	May	Jun.	Jul.	Aug.	Sept.	Oct.	Nov.	Dec.	Total
ALO	NILU001	3	10	3	2	0	0	0	0	0	1	3	3	25
ALO	NILU002	2	10	2	1	0	0	0	0	0	0	3	2	20
DDU	CNRS.SA007	0	0	0	0	0	0	0	0	0	0	0	0	0
DDU	RMR_CNRS.SA002	0	0	0	0	0	0	0	0	0	0	0	0	0
ESR	UBONN003	0	2	6	0	0	0	1	5	0	0	0	0	14
EUR	CARE.EC.STB001	0	5	3	0	0	0	0	0	0	0	0	0	8
EUR	CARE.EC.STB002	0	5	3	0	0	0	0	0	0	0	0	0	8
HOH	DWD001	6	7	7	16	9	3	8	10	7	7	8	10	98
HOH	DWD002	6	7	8	16	9	3	8	10	8	7	8	10	100
LAR	LPA001	0	0	0	0	0	0	0	0	0	0	0	0	0
LAR	LPA002	3	8	17	15	19	20	21	24	15	14	20	15	191
LAU	RIVM002	6	4	6	5	6	5	5	6	3	4	6	4	60
LAU	RIVM003	0	0	0	0	0	0	0	0	0	0	0	0	0
MLO	NASA.JPL001	8	8	9	11	10	10	14	14	9	11	8	1	113
MLO	NASA.JPL002	8	8	9	12	10	11	14	14	9	11	8	2	116
NYA	AWI001	0	0	0	0	0	0	0	0	0	0	0	0	0
NYA	AWI002	0	0	0	0	0	0	0	0	0	0	0	0	0
OHP	L_CNRS.SA001	15	14	6	6	2	0	8	10	8	11	10	13	103
OHP	r_CNRS.SA001	6	17	16	15	17	16	1	0	18	20	16	10	152
RGA	CEILAP001	2	2	3	0	0	0	1	6	4	6	3	2	29
TMF	NASA.JPL003	2	2	4	8	10	5	4	10	1	7	5	7	65
TMF	NASA.JPL004	2	2	4	8	10	8	0	10	4	10	10	7	75
TSU	NIES001	3	7	4	1	0	0	0	1	0	2	4	4	26
TSU	NIES002	3	6	3	1	0	0	0	1	0	2	4	3	23
TOTAL all systems		75	124	113	117	102	81	85	121	86	113	116	93	1226

Note that submissions of data for Dumont d'Urville (temperature), Ny Ålesund (temperature and ozone) and Lauder (temperature) are still foreseen.

Table 14-7: Data submission statistics, 2008 (in gray temperature lidar systems)

Station	System	Jan.	Feb.	Mar.	Apr.	May	Jun.	Jul.	Aug.	Sept.	Oct.	Nov.	Dec.	Total
ALO	NILU001	9	3	0	0	0	0	0	0	0	0	0	0	12
ALO	NILU002	0	0	0	0	0	0	0	0	0	0	0	0	0
DDU	CNRS.SA007	0	0	0	0	0	0	0	0	0	0	0	0	0
DDU	RMR_CNRS.SA002	0	0	0	0	0	0	0	0	0	0	0	0	0
ESR	UBONN003	0	0	0	0	0	0	0	0	0	0	0	0	0
EUR	CARE.EC.STB001	0	7	4	0	0	0	0	0	0	0	0	0	11
EUR	CARE.EC.STB002	0	7	4	0	0	0	0	0	0	0	0	0	11
HOH	DWD001	9	9	5	7	8	7	7	9	5	9	8	5	88
HOH	DWD002	9	9	5	7	8	7	7	9	5	9	8	6	89
LAR	LPA001	0	0	0	0	0	0	0	0	0	0	0	0	0
LAR	LPA002	5	13	0	6	17	8	0	7	16	11	24	14	121
LAU	RIVM002	6	5	6	6	4	5	2	6	6	6	5	4	61
LAU	RIVM003	0	0	0	0	0	0	0	0	0	0	0	0	0
MLO	NASA.JPL001	10	7	15	10	14	12	12	14	13	7	8	10	132
MLO	NASA.JPL002	10	7	15	10	14	12	12	14	13	7	8	10	132
NYA	AWI001	0	0	0	0	0	0	0	0	0	0	0	0	0
NYA	AWI002	0	0	0	0	0	0	0	0	0	0	0	0	0
OHP	l_CNRS.SA001	9	5	11	11	4	0	0	0	0	0	0	0	40
OHP	r_CNRS.SA001	8	17	12	4	0	0	0	8	13	12	9	9	92
RGA	CEILAP001	0	1	1	3	1	1	0	2	7	11	4	1	32
TMF	NASA.JPL003	7	11	7	16	9	4	10	10	7	4	3	6	94
TMF	NASA.JPL004	7	11	8	16	9	4	11	11	7	12	5	6	107
TSU	NIES001	2	5	1	1	1	0	0	0	0	0	0	0	10
TSU	NIES002	2	5	1	1	1	0	0	0	0	0	0	0	10
TOTAL	all systems	93	122	95	98	90	60	61	90	92	88	82	71	1042

Note that submissions of data for Alomar (temperature and ozone), Esrange (temperature), OHP (ozone), Dumont d'Urville (temperature), Ny Ålesund (temperature), Lauder (temperature), Tsukuba (ozone and temperature) are still foreseen.